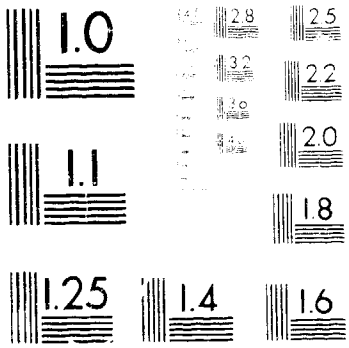

NASA CONTRACTOR REPORT

NASA CR-168027

NASA

EXPERIMENTAL STUDY OF THE THERMAL STABILITY OF HYDROCARBON FUELS

By Pierre J. Marteney
Meredith B. Colket
Alexander Vranos

Prepared by
UNITED TECHNOLOGIES RESEARCH CENTER
East Hartford, CT 06108

For
NATIONAL AERONAUTICS AND SPACE ADMINISTRATION
LEWIS RESEARCH CENTER
CLEVELAND, OHIO 44135
DECEMBER 1982

Report CR-168027

Experimental Study of The Thermal Stability of Hydrocarbon Fuels

Contractor Report

Pierre J. Marteney
Meredith B. Colket
and
Alexander Vranos

United Technologies Research Center
East Hartford, CT 06108

Work Performed For

NASA-Lewis Research Center
Cleveland, Ohio 44135

Under Contract NAS3-22511

Stephen Cohen, Project Manager

Experimental Study of The Thermal Stability of Hydrocarbon Fuels

TABLE OF CONTENTS

SUMMARY

The thermal stability of two hydrocarbon fuels (premium diesel and regular diesel) was determined in a flow reactor under conditions representing operation of an aircraft gas turbine engine. Temperature was varied from 300 to 750 F (422 to 672 K) for fuel flows of 2.84 to 56.8 liters/hr (corresponding to 6.84×10^{-4} to 1.63×10^{-2} kg/sec for regular diesel fuel and 6.55×10^{-4} to 1.37×10^{-2} kg/sec for premium diesel fuel); test times varied between 1 and 8 hr. The rate of deposition was obtained through measurement of weight gained by metal discs fixed along the channel wall. The rate of deposit formation is best correlated by an Arrhenius expression, $R = \exp(-E/R\bar{T})$, where E is approximately 12 kcal/mole, and $\bar{T}$ is an average of wall and bulk-fluid temperatures.

The sample discs in the flow reactor were varied among stainless steel, aluminum and brass; fuels were doped with quinoline, indole and benzoyl peroxide to yield nitrogen or oxygen concentrations of approximately 1000 ppm. The most substantial change in rate was an increase in deposits for brass discs; other disc materials or the additives caused only small perturbations.

Tests were also conducted in a static reactor at temperatures of 300 to 800 F (422 to 700 K) for times of 30 min to 2 1/2 hrs. Much smaller deposition was found, indicating the importance of fluid transport in the mechanism.

As-received and stressed fuels were examined by liquid chromatography; within the limits of detection, no difference was found. Deposits from both flow and static reactors were also examined. The major finding was the presence of halogens, particularly chlorine, and an association with increased deposition.

INTRODUCTION

The tendency of petroleum distillate fuels to form deposits on heated surfaces has long been recognized as a problem, particularly in aircraft gas turbine engines, where deposits may form in manifolds or nozzle passages. Although limited coking has been tolerable in many areas, the dependence of deposition on temperature and fuel composition calls for a thorough understanding of the mechanisms of formation if anticipated engine modifications and possible fuel variations are to be acceptable.

Modifications to engine operation are projected to include two changes; increase in combustor inlet temperature and prevaporization of fuel. Probable changes in fuel composition tend toward a greater fraction of aromatics and olefins, plus increase in minor species such as sulfur or nitrogen. These factors combine to make thermal stability a serious concern. On one hand, the critical passages are bathed in hotter compressor air; added to this, higher flame temperatures may, through several mechanisms, lead to higher thermal loads on nozzles. On the other hand, these potential fuels, coming from new sources or being produced by changes in refining techniques, may have innately-lower stability at any temperature.

The present studies represent a continuation in the fuel stability program sponsored by the Lewis Research Center of NASA. Under the first of two contracts, UTRC studied the thermal stability of Jet A and No. 2 Home Heating Oil. In the present program, regular and premium diesel fuels were tested. The fuel properties now tested cover a broad spectrum, particularly in aromatic content, ranging from 22 percent to 48 percent aromatics.

The present flow-reactor tests were undertaken with two goals: to determine the individual coking rate of each of the two test fuels, and to obtain a greater understanding of the general mechanisms of deposition. To attain the first, tests were conducted at conditions similar to those used in previous studies. To attain the second, disc material and position across the channel were varied, runs were conducted with two materials at a single location, fuels were doped with scavengers or inhibitors, and total mass throughput was held constant at varying flowrate.

Static-reactor tests were conducted to determine the importance of transport or replenishment of fuel in deposition. Analyses of deposits and fuels were conducted in an attempt to identify prominent species or possible paths of reaction.

EXPERIMENTAL

Flow-Reactor Tests

The apparatus used in these tests was constructed under a previous contract (NAS3-21593), and was used with minor modifications. The test system, shown in Fig. 1, included a 275 gal storage tank, delivery pump, and the test assembly; the fuel preheater was used to raise the inlet fuel temperature for specific tests. The flow control system and a steam heater were adjacent to the simulator in a test cell; the data console was in an adjacent control room. The entire test system was independent of all other units in the test area.

The fuel was delivered to UTRC in two lots of 15 drums (325 gal) each. The fuel was supplied to NASA order by Amoco Oil Company, Whiting, Indiana, as Item #23109, "Furnace oil, no additive," and Item #23315, "Diesel Fuel, no additive." For consistency with the intent of NASA, these were termed Regular Diesel Fuel and Premium Diesel Fuel, respectively.

The two fuels differed in two respects. The premium diesel fuel was a straight-run fuel, whereas the regular fuel was a mixture of cracked and straight-run components. In addition to the difference in aromatic content, 19.47 percent (premium) vs. 47.8 percent (regular), the overall balance of the two fuels varied. As-received fuel properties are described in Appendix A. Fuel was transferred from barrels to the 275 gal. tank as needed. Flow through the test system was controlled at 300 psig (2×10^6 Pa), and was regulated by Hago oil-burner nozzles rated at 0.75 to 15 gph (2.84 to 56.78 l/hr) installed at the outlet of the test channel. Flow was monitored by turbine meters in the inlet line and by direct volumetric measurement of fuels collected at the outlet.

The tests were conducted in the fuel-system simulator (Figs. 2,3) at 300 F to 750 F (422 to 672 K). The internal passage is 0.10 x 1.12 x 24.75 in (.0025 x .028 x .629 m); on the 1.12 in dimension, sample discs of 0.75 in (.019 m) diameter were placed at distances of 1.5, 8.5, 15.5 and 22.5 in (.038, .216, .394, and .571 m) along the channel. Discs were fixed at the wall during test runs, then removed and examined; deposit weight was found by difference.

For some of the tests, two modifications to previous procedure (Ref. 1) were adopted. In the first, two semi-circular samples were mounted at one location to determine the effect of variation in material while including a reference material. In the second change, discs were fabricated with short mounting legs and were positioned midway across the channel, so that flow passed over both faces. This mounting was intended to determine the relative effect of bulk vs. wall temperature on coking rate.

The sample discs for a given run were cleaned and weighed before mounting. Materials and approximate initial weights for full-circle discs were: stainless steel, 0.34 g; aluminum, 0.24 g, and brass 0.46 g. (Weights are not proportional to specific gravity, because different thicknesses were available).

Run temperature was set at the controller; heat-up time varied with flow and run temperature, but was typically 15 to 20 min to 625 F (603 K). Run parameters were printed automatically every 10 minutes or manually on demand. The length of a run was obtained by interpolation of times corresponding to temperatures falling within 20 F (11 K) of the specified run temperature. Because of the strong dependence of coking rate upon temperature, lower temperatures are insignificant in coking for a given run; heating and cooling within this band together correspond to less than 10 min in a run at 625 F (603 K). The time error in a three-hour run is no greater than approximately 5 percent.

At the conclusion of a run, the specimen discs were removed, washed in a 1:1 mixture of hexane and benzene, dried and weighed. Weight gains varied with condition, but were typically of the order of 100 µg (0.0001 g). Reproducibility of weight differences was found to be approximately 5 to 10 µg. The analytical error therefore is approximately 10 percent; the absolute value, however, is a strong function of weight gain, and is in essence a function of run temperature.

Static-Reactor Tests

The flow-reactor tests were designed to simulate conditions present in a fuel system of a combustor, but with enhanced control and flexibility of temperatures, surfaces, etc. Calculations (of fluid temperatures vs. distance, for example) demonstrated that further manipulation of experimental conditions was desirable, and laboratory-scale, static-reactor tests were performed to provide greater variation, specifically of temperature, surface, and fuel preparation.

Several preliminary designs for the static reactor were constructed and tested. Tubes sealed with preweighed stainless steel strips and fuel were inserted into a tube furnace and heated for periods of 1/2 to 3 hrs. For these tests, heat-up times were 10-15 min, and the tubes were prone to leaking. In the final tube design, leaking of fuel was minimized by partially filling the tube with fuel to account for its expansion and by using double-ferrule (Swagelok) caps. Heat-up times were minimized through resistive heating. Deposits were collected on preweighed stainless steel strips inserted into the tube. Weights of all samples were determined by difference; for some of the samples, chemical compositions were determined (see Appendix B for description of the techniques). The results of the chemical analysis are described in a separate section.

The static reactors were constructed of 304 stainless-steel tube, 0.375 in (.0095 m) O.D., 0.305 in (.0077 m) I.D., and 3.5 in (.0889 m) long. Electrical contacts were silver-soldered onto the end caps. Three Chromel-Alumel thermocouples were spot welded to the outside wall of the tube. They were located approximately 0.75, 1.75 and 2.75 in (.019, .044 and .069 m) from one end of the tube, and were electrically floated to prevent spurious readings; thermocouples were not placed directly in the liquid fuel. Typically, the wall temperature was increased from room temperature to run temperature within about 20 seconds. For example, for a final temperature of 603 K, about 500 watts (300 amps at 1 to 2 V) was initially passed across the tube. The power was then rapidly decreased to a steady-state level of about 20 watts (55 amps at 0.35 volts) to maintain constant temperature. Typical temperature histories for the three thermocouples are shown in Fig. 4. After the test period, the electrical contacts were discontinued and the tube was quenched in water. Times for cool-down were typically 3 to 5 minutes.

Prior to testing, the tubes were cleaned by a variety of techniques; these included scrubbing with a test-tube brush and rinsing with methylene chloride, scrubbing the interior walls with steel wool, acid cleaning, and ultrasonic cleaning with a mixture of ammonia and hydrogen peroxide. Unless specified otherwise in the summary of static-reactor results, (Table 2), the tubes were brushed and cleaned with methylene chloride. Type 316, stainless steel strips, .171 in x 3.5 in (.004 x .089 m), scratch-free and cleaned with methylene chloride, were preweighed to the nearest microgram; initial weight was approximately 0.62 grams. Measurements of cleaned strips could be repeated within 2 micrograms.

The internal volume of tubes was approximately 4.5 ml. The amount of fuel placed in the tube for the test was determined by estimating expansion of the fuel and allowing for approximately 5 percent of the reactor volume for gas-phase species (compressed air plus fuel vapor). It is important to allow for expansion of the liquid, since an increase in volume as great as 50 percent can be expected, and extreme pressures would be produced at elevated temperatures. For a run at 603 K, the 5 percent void limits the run pressure to 340 psia (2.3×10^6 Pa).

Following the run, the stainless steel strip was removed, rinsed in a 1:1 hexane/benzene solution, heated for one-half hour at 373 K, cooled to room temperature and weighed. If weighing was delayed, the strips were reheated prior to weighing; otherwise the weight gain was biased by adsorption of gases or moisture from the atmosphere.

An equivalent deposit thickness was calculated using the measured deposit weight. It was assumed that the specific gravity of the deposit was 1.8 (based

on UTRC measurements of combustion-derived soot) and that the deposit was uniformly distributed on the substrate. Although the surface may appear to be uniformly covered, photographs taken in the electron microscope reveal that the surface is highly irregular. In some areas, the substrate is essentially bare; elsewhere, discrete and heavy deposits are formed. The calculated deposit thicknesses presented in this report are useful in indicating that a relationship between weight and minimum thickness exists, but they are intended to be only descriptive.

RESULTS AND DISCUSSIONS

Flow-Reactor Tests

The major test program was conducted in two parts, both conducted in the fuel system simulator. In the first part, 45 tests were conducted using regular diesel fuel; in the second part, 35 tests were conducted using premium diesel fuel. Runs were conducted at 300 to 750 F (422 to 672 K) at flow rates of 2.84 to 56.8 l/hr (corresponding to 6.84×10^{-4} to 1.63×10^{-2} kg/sec for regular diesel fuel and 6.55×10^{-4} to 1.37×10^{-2} kg/sec for premium diesel fuel) with both neat and doped fuels. A tabulation of the as-received fuel properties is given in Table A-1. Quinoline and indole were added to increase the nitrogen concentration to 1000 ppmw; 1 percent by weight benzoyl peroxide was added to yield oxygen at 1300 ppmw. Fuel was also preheated and deoxygenated before use. However, those treatments were applied only to the regular diesel fuel; premium diesel was tested as-received. Tests for which the results are included in this report are listed in Table 1. Test conditions for regular diesel fuel were varied somewhat more widely than for premium fuel, to allow better comparison with data from previous tests of Jet A and No. 2 HH oil (Ref. 1).

The experimental variables, in order of importance, had previously been shown to be wall temperature, flow rate and time (Ref. 1). In these experiments, as in previous tests, the wall temperature is fixed and remains constant with both flow rate and time, because the heat input and heat capacity of the structure are large compared to the heat load imposed by the fuel. Changes in flow rate affect both the heating rate of fuel and the type of flow, i.e. laminar or turbulent. In these tests, the flow is, for the most part, laminar; although transition to turbulent flow should occur at the higher mass flows, the transition is probably delayed because of the very-smooth walls and addition of heat from the surface (Ref. 2). This was also found in other tests recently conducted at UTRC (Ref. 3). Within the envelope of laminar flow, the principal affect of increased velocity is in reduction of the fluid temperature rise. The probability that two types of reactions, viz, liquid-phase and wall, are responsible for deposit formation suggests that the temperature under which each occurs is most important. For that reason, the results reported here are examined in light of bulk fluid temperature and wall temperature, and flow rate is not specifically considered.

Regular Diesel Fuel

A summary plot of results for neat regular diesel fuel is given in Fig. 5, in which the "local" coking rate is shown for each of the four disc positions. Data points are segregated only by wall temperature; flow rate, disc material, or other variation is not shown.

The general trend of coking in regular diesel fuel, as shown in Fig. 5, is an increase with temperature. However, the increase is not uniformly proportional at all disc locations. To illustrate this point, the data are segregated by temperature in Figs. 6-8. At 300 F (422 K) (shown in Fig. 6), the variation in deposition along the channel is small, although a maximum appears to occur toward the end of the channel, at about the third disc. At 500 F (533 K) (Fig. 7) the deposition varies even more, and the maximum is nearer the inlet. At 625 F (603 K) (Fig. 8), the maximum occurs even nearer the entrance, and the variation along the channel is still greater. The single run at 750 F (672 K), (not shown) is in agreement with the trend from lower temperatures; the maximum lies at (or before) the first disc. These results are in excellent agreement with those of Ref. 1, shown in Fig. 9.

In previous analyses of coking data (Ref. 1), results were correlated only with the wall temperature. An alternative approach has been taken for these data, and additional insight results.

A typical Arrhenius plot showing coking rate vs. the reciprocal of wall temperature, Fig. 10 (from Ref. 1) or Fig. 11 (from the current tests), would lead to the conclusion that two mechanisms are in effect, that they may be independent, and that they have different dependence on temperature. If coking were strictly related to surface reactions, deposit rate from all four discs in a single run would be the same, since wall temperature is constant (except for very small center-to-end variation); this is clearly not the case in Figs. 6-8. On the other hand, if the deposition were strictly related to fluid temperatures, then a plot of rate as a function of "local" fluid temperature should fit not only all four points from a given run but points from all runs. As a test of this point, the local fluid temperature was calculated for all nominal run conditions (see Appendix C) and has been used in analysis of the data.

An Arrhenius plot of local rate vs. reciprocal of calculated local bulk temperature is shown in Fig. 12 for a wall temperature of 500 F. The indicated dependence on temperature is now negative; that is, deposit rate decreases with increasing fluid temperature. Since it is clear that a generally-positive dependence on temperature exists (as shown in Fig. 11), the bulk temperature alone may not be used.

An alternative approach, consistent with the assumption that two processes are at work, is to compose the Arrhenius plot using the average value of T_{wall} and T_{bulk}; the result is given in Fig. 13. An activation energy of 12 Kcal/mole is a reasonable representation of the data for all stainless-steel discs (shown by open circles). The data for brass (open squares) clearly lie above those for stainless, and appear to match an activation energy of 5 Kcal/mole. As shown in the section on premium diesel fuel, paired half-discs (brass and stainless) in the same location differ by a factor of as much as eight

in deposition rate; this can only be ascribed to a surface phenomenon, since all other conditions are the same. The difference in deposition rate between stainless steel and brass surfaces could be due to different mechanisms, or it might be a result of similar reactions at a different number of sites. In Fig. 13, a line representing an activation energy of 6 Kcal/mole could be drawn for stainless-steel discs at lower temperatures, matching the slope for brass within experimental error. This would then indicate similar mechanisms are in force; these estimates are in agreement with a value of 6.5 Kcal/mole derived in Ref. 8. Data for stainless steel at higher temperatures are then fit by a line corresponding to 22 Kcal/mole. The alternative, single-slope fit of 12 Kcal/mole is a possible correlation, but it is a somewhat poorer fit.

The dependence of coking on other factors can also be seen in Fig. 13. Data for aluminum discs are shown as triangles; the data are scattered approximately as for stainless steel, and the rate may be said to be about equal. However, in the case of doped fuels (all treatments as a class), the data lie below those for neat fuels. The expectation was that doping or preheating would accelerate the rate of deposition. Although a line is not fit to the treated-fuel data, it is possible to argue for a line representing an activation energy of about 12 Kcal/-mole, with a deposition rate lower by approximately 30 percent at all temperatures.

Premium Diesel Fuel

Tests with premium diesel fuel were conducted within a narrower temperature regime than for regular diesel fuel; the bulk of testing was conducted at 625 F (603 K). Two innovations in technique were developed. First, in place of a single disc, two half-discs were mounted in each sample location, so that the effect of material at each station could be determined. Second, an additional disc was mounted midway across the test channel (with flow over both faces) to probe the effect of bulk vs. wall temperature.

The rate of deposition in premium diesel fuel at 500 F (533 K) is shown in Fig. 14. Two runs were conducted; the mean value for regular diesel fuel (from Fig. 7) is also shown. The difference in rates is probably within experimental error.

Deposition on stainless-steel discs at 625 F (603 K) is shown in Fig. 15. The bulk of the data were taken using one nozzle, with an average flow rate of 2.42 l/hr. A mean value is shown, and the comparable value for regular fuel is included. Note that the coking rate in premium diesel is, on average, about 25 percent smaller.

The results for paired, split discs are given in fig. 16. These runs were conducted under similar conditions of temperature and flow. The mean value for stainless discs (from Fig. 15) is also shown. Data for stainless-steel half discs, although scattered, reasonably fit the mean value; aluminum produces nearly the same deposit rate. The effect of brass discs is pronounced; on average, the rate for brass is a factor of nearly two greater than for stainless. The enhancement in rate is particularly noticeable for the later discs. At the inlet, the difference is not more than 30 to 50 percent, while at the third or fourth disc the difference may be a factor of five.

The difference found between stainless and brass can be attributed to the presence of specific surface reactions, since the channel is the same for both species. The importance of bulk temperature may be reflected in the growing difference on brass; as the temperature rises, species which lead to deposition are produced, yet reaction with the wall is required. When the temperature is low (as at the inlet) no difference would be found; as the temperature rises, the more-reactive surface gives higher deposits.

Results for discs suspended at midchannel are shown in Figs. 17 and 18. In Fig. 17, coking on the tabbed discs is shown; a schematic drawing of the support and position is shown on the figure. The average rate is higher than the grand average for wall mounted discs of (Fig. 15), but these tests were conducted exclusively at lowest flow rate, (2.84 l/hr), and higher deposition rates are to be expected at the higher average temperatures.

The tabbed discs were used in tests of fuel preheated to 300 F (422 K), and the results are shown in Fig. 18. In these runs, both tabbed and normal discs were installed for more-detailed comparison. The rate for both discs and tabs is slower in preheated fuel, and the rate for tabs is below that of discs. The normal, wall-mounted discs are at the same temperature whether fuel is preheated or not, whereas the midspan discs become significantly hotter, although still not attaining the wall temperature. The only mechanism by which preheating can interact as shown is by a depletion of species which normally initiate or participate in reactions leading to deposition. Although the data are not plotted, the same trend was found for stainless vs. brass split discs in the case of room temperature vs. preheated fuel; the rate was reduced by heating, and, more important, the rate was further reduced by additional preheating to 338 F (443 K). In the case of brass discs in the normal and midspan positions, the midspan discs showed lower deposition, but the preheating yielded only a small effect. This may be due to the higher reactivity of the brass surface.

In summary, the premium diesel fuel is characterized by somewhat lower deposition than the regular diesel fuel. Detailed tests in which surfaces and locations were varied show a major increase in deposition on brass, but a nearly-

negligible difference on aluminum. Preheating of fuel reduces coking on steel or aluminum, but has a small effect on brass. These results and those for regular diesel fuel are consistent with the supposition that both liquid and surface reactions are important in deposit formation. From the results on regular fuels shown in Fig. 11, it may be inferred that one group of reactions dominates to a wall temperature of approximately 550 F (560 K) and is characterized by an activation energy of approximately 6 Kcal/mole, while a second class of reactions dominates above that temperature and has an activation energy of about 20 Kcal/mole. On the basis of studies with paired and midstream mounted discs, it is concluded that the lower temperature reactions are surface-related and the higher-temperature reactions are liquid-phase phenomena. Moreover, the activation energies in the two regimes are in agreement with such a hypothesis, i.e., surface or surface-catalyzed reactions would be expected to require less energy.

Static-Reactor Tests

A summary of the static reactor tests using the final tube design and heating method is listed in Table 2. All of the tabulated tests were conducted at 603 K using regular diesel fuel. For each run, the amount of fuel was 2.7-2.8 ml. The fuel remaining after the test was generally measured to be 2.3-2.5 ml; the difference is predominately due to fuel retained on the walls of the measuring graduated cylinder and within the reactor itself. Recovery of less than this amount indicated leakage during the run.

Highest deposits were produced when new fittings were used, as shown by Runs 63, 67 and 74. On subsequent use, the deposits produced in a given tube rapidly decreased. For runs with new fittings, the heated fuel appeared cloudy, and the end caps seemed to be cleaner than unused end caps (which had been silver-soldered to the electrical connectors). The deposits were analyzed by Auger Electron Spectroscopy to determine whether the presence or absence of any particular species could be correlated with the deposit weight. (The technique and results are described elsewhere in this report.) It was found that high deposit weights were associated with high chlorine content in the deposit.

To determine whether the chlorine was present in the metal system, the interior surfaces of the tubes and fittings were examined using the scanning electron microscope (SEM). The technique does not isolate the surface of the sample; instead, the SEM examines a volume-average of material to depths of 1 to 2 microns. Because of the averaging, surface contamination occurring only within the first several atomic layers may not be resolved. The SEM examination revealed:

1. Unused tubes and fittings show no trace of chlorine, regardless of cleaning techniques. Traces of sulfur are found in new fittings.

2. Used tubes clearly show traces of chlorine, regardless of cleaning technique.

3. Fittings which have been silver-soldered (for electrical connections), show traces of chlorine as occasional spots on the metal surface, although chlorine is not present in the solder flux.

These results suggest that the chlorine may have been accumulated by handling and fixed to the surface during soldering. However, chlorine was found in deposits from earlier tubes on which no silver soldering was done. Although some of the chlorine may be produced from salt deposition during handling, much of the chlorine detected is independent of salts, since AES analysis indicated that alkali metals (sodium or potassium) were not jointly present. Consequently, the source of chlorine appears to be the fuel, but new surfaces appear to accelerate deposit-forming reactions with chlorine.

The importance of chlorine and its effect on the deposit weight was demonstrated further by ultrasonically cleaning new tubes in 1:1 solution of ammonia and hydrogen peroxide. It is believed that most of the chlorine present on the walls of the tube was removed by this technique. For Run 76, no deposit was observed after one hour of heating at 603 K, despite the presence of a blanket of air over the fuel. Although not shown in Table 3, identical results were obtained when using preliminary reactor designs and ultrasonic cleaning; the possible link to chlorine removal was not evident at that time. It is also possible that this ultrasonic cleaning technique prepares the surface to inhibit coke deposition; however, the primary effect appears to be removal of chlorine from the surface.

In Runs 75, 79, and 80, trichloroethylene was added to the fuel prior to testing to investigate the effect of liquid-phase contamination by chlorine. The results from Run 75 are most dramatic. For this experiment, 1 percent or 10,000 ppm by volume of trichloroethylene was added to the fuel, and deposit of 801 micrograms was formed. This result compares to Run 76, with no additive, for which no coke was measured (± 2 micrograms). In Run 79, only 200 ppm by volume was added but a measurable increase over the blank run (Run 76) was still found. In Run 80, approximately 1500 ppm was added. The measured deposit is smaller than would be expected on the basis of Run 75 and 79, but this may be due to a small leak (experience established that leaks diminished the deposit weight).

A comparison of Runs 74 and 78 demonstrates the strong effect that a new end cap have on the total weight produced, even when it is ultrasonically cleaned prior to use. Run 77 was performed to examine the effect of acid (HCl) treatment

of the reactor walls. Prior to acid exposure, the tube was cleaned ultrasonically to remove traces of chlorine. The deposit formed during this test was small, but noticeable. Additional testing should be performed to examine this effect.

Further discussion of these results are presented in the following section of this report, in which AES results are described and static reactor data are compared to flow reactor data.

CHEMICAL ANALYSIS OF FUELS AND DEPOSITS

Task II of this contract specified studies of fuels and deposits. As a starting reference, the overall composition and physical properties of the two test fuels were determined by ASTM methods for aircraft fuels, and are presented in Appendix A.

The intent of Task II was to characterize the chemical properties of the fuels, then to determine the relationship between deposition and composition or changes in composition during stressing in the flow reactor. The Fuel Chemistry Laboratory concentrated on refinement of techniques in liquid chromatography (LC), including methods for characterizing major classes, including polar and non-polar fractions, aromatics, olefins and aliphatics, and detection of the spectra within these groups. Chromatograms illustrating the sensitivities of the techniques are shown in Figs. 19 and 20. In Fig. 19 is shown a liquid chromatogram in which aromatic ring compounds are separated into 1-, 2-, 3- and 4-ring species. The separation was carried out on an aminopropylsilane column with an ultraviolet detector. The sum of areas corresponds to approximately 48 percent of the fuel; the peak marked NAP, which is the double-ring naphthalene compounds, represents nearly 9 percent of the fuel.

Separations of fuels before and after stressing were conducted, and chromatograms were compared in detail. Irrespective of stressing conditions, changes were not detected. This is consistent with the experimental result that the deposit weight represents of the order of one part in a million of the fuel. The result also suggests that no single species is responsible for the formation of deposits.

A second chromatographic technique was also used. Gas chromatography with flame-ionization detection (GC/FID) was employed. In this technique, individual molecular peaks are detected, the area of each peak is measured and compared to tabulated standards, and the concentration of each species is tabulated. A section of a GC/FID spectrum is shown in Fig. 20. The peak designated 14.11 (the retention time in minutes) corresponds to a C_{16} molecule, and is 3.73 percent of the sample. Subject to experimental conditions, individual peaks corresponding to 100 ppm can be resolved.

Fuels were extensively tracked by the GC/FID method; however, as in the case of the LC technique, changes in composition were not detected after any tests in the flow reactor. It was partly for this reason that the static reactor tests were initiated; to run under conditions which might force major reactions to occur, and primary emphasis was shifted to analysis of the deposits.

The analytical techniques used for deposit analysis were conducted under two constraints: 1) only small quantities (as little as 100 micrograms) were available; and 2) the deposit often was insoluble in a variety of solvents, and mechanical removal (i.e. scraping, etc) proved to be difficult. Chemical analysis was obtained predominantly via Auger Electron Spectroscopy (AES), although a few samples from the flow reactor were analyzed using ISS/SIMS for comparison. The AES and ISS/SIMS techniques are both described in Appendix B.

Flow-Reactor Deposits

Typical AES analysis of deposits produced in the flow reactor are shown in Figs. 21 and 22 for Run 9 (Disc 33, SS) and Run 25 (Disc B9, Brass), respectively. Both deposits were obtained in runs at 500 F (533 K) for 3 hours; the run profiles are shown in Fig. 23. The analyzed discs were both mounted at the first position in the reactor. Gravimetric analysis indicated that the brass disc collected nearly eight times as much deposit (this was approximately true for all disc positions in the two runs). Deposit thickness was estimated assuming the specific gravity of the deposit to be 1.8, with uniform distribution of the deposit.

Despite the similarity in run conditions, there are significant differences between the two discs: the abundance of chlorine on the brass disc and the discrepancy in carbon concentration. On the brass disc, major species are chlorine (~ 35 percent), oxygen (~ 35 percent), carbon (~ 15 percent) and sulfur (~ 15 percent); on the stainless steel disc, carbon is dominant (~ 95 percent), and oxygen and sulfur make up the balance.

Part of the apparent difference in composition may be artificial because of the morphology of deposits. Typically, the earliest deposits are flat, while heavy deposits appear as discreet lumps. A technique such as AES may be biased by shallow deposits not covered by the lumps; it is not possible to give the absolute depth at which a given species is found. From the data of Figs. 21 and 22, it cannot be concluded that chlorine is present throughout the deposit on brass. In fact, chlorine may be present on the metal surface in both cases, but may not be apparent if the deposit over stainless steel is very uniform.

Analysis of other flow-reactor discs and static-reactor strips indicated that chlorine was also found over stainless steel substrates and, when chlorine was present, the relative concentration of carbon was low and that of other atoms, particularly oxygen, was high.

For comparison, analysis of deposits from discs 33 and B9 was obtained at a depth of 25 Å using ISS/SIMS. The ISS method provides only relative atomic

ratios; these values are compared with those from AES data in Table 3. Agreement between the two analytical techniques is poor. As in the case of AES, surface contamination still significantly perturbs profiles, and concentrations may be changing rapidly with depth. Furthermore, there is a difference in the estimated depth (due to sputtering) for the two methods. Considering these uncertainties, the discrepancies in the sets of data are understandable. The relative values obtained using AES are believed to be more reliable due to better repeatability and quality of data. SIMS data using both $^{20}Ne^-$ and $^{20}Ne^+$ were obtained and are shown in Figs. 24 and 25 for Runs 9 (disc 33), 25 (disc B9), and 29 (disc B13). As discussed in the description of the SIMS technique, these data at best are primarily qualitative, and detailed concentration data should not be expected from these mass profiles. Negative-ion bombardment (Fig. 24) showed greater sensitivities to non-metals and to ions with relatively-low negative ionization potentials. Chlorine appears very strongly in Run 25, consistent with AES analysis, which showed chlorine to be present at concentrations up to 38 percent. Since the ratio of mass 35 to 37 is the same as the naturally-occurring ratio for Cl^{35}/Cl^{37}, the identification of chlorine as a contaminant in the deposit is unambiguous. In Run 25, a small amount of fluorine is found; more surprising is the strong fluorine signal in Run 29. For Runs 26 to 34, fuel was blended with quinoline and stored in a 75 liter tank which had originally contained Freon-11. The tank was used because it seemed especially clean, and it had been additionally cleaned and rinsed with neat fuel prior to use. Remnants of fluorocarbons remaining on the tank were presumably sufficient to affect the character of the deposition. Incorporation of halogens in the deposits suggests an influence by the halogen on deposit mechanism or rate. However, the source may still be unknown. In the case of the doped fuel, the empty drum would have had, at the most, a thin residue of Freon-11 on the wall: no liquid Freon-11 was present. After rinsing and dilution by the doped fuel, the concentration of fluorine could not have exceeded a few ppm, and the fluorine concentration would require enhancement by several orders of magnitude during deposition to yield the observed concentration. The positive ion data (Fig. 25) are more sensitive to metals; hydrocarbons do appear in these data, but the most prominent features are metals, especially Na, Al, and K. The peak heights are a greater reflection of their low ionizing potential than of concentrations. No evidence for these species was observed in the AES results; this suggests that upper concentration limits are 2.5 percent for sodium and less for all others. Additional work on the importance of metals in coke deposits was not attempted, since it is reasonable to find these species at such concentrations as a result of handling.

Another series of analyses was performed on deposits from adjacent half discs: #181 Stainless and #181 Brass, both from Run 121. These deposits were formed simultaneously under identical conditions in the flow reactor; the only

difference is the substrate materials. Depth profiles, including concentration of the substrate material, are shown in Figs. 26A and B. Clearly, iron and copper represent the disc material; surprisingly-high concentrations of these materials are measured near the surface of the deposit in spite of relatively-heavy deposition. Although some diffusion of the substrate into the deposit may occur, the apparent presence of the substrate within the deposit is likely an artifice of the measurement technique and the character of the deposit. If the deposit is not distributed uniformly over the disc material, the substrate material will appear to be mixed with the deposit. If the deposit is uniform, the substrate will be hidden. In addition, the sputtering used to ablate the surface (for depth analysis) may preferentially remove or redeposit certain atoms. If Figs. 26A and B were renormalized without the substrate material, other concentrations would rise uniformly.

The major difference between the deposits over brass and stainless steel from Run 121 is the relative sulfur concentration. Over the brass disc, sulfur accounts for 50 percent of the deposit; on stainless steel, sulfur represents only 10 percent of the deposit. Fluorine also appears over the stainless steel, but no trace was observed over the brass sample. The fluorine signal is nearly coincident with a peak from iron; as the iron concentration increases, it masks the signal from fluorine.

At this time, there is no explanation for these rather substantial differences in the coke deposited simultaneously over stainless steel and brass. These differences demonstrate a need for the understanding of fundamental chemical and physical processes occurring during formation of deposits. The only clear message that these data provide is that halogens (or possibly polar compounds in general) may significantly affect the character of the deposit. Apparently, trace concentrations of such species may significantly alter the character of the deposit and the amount of the deposit. In addition, the substantial differences observed in the deposits over dissimilar half discs suggest that surface composition or contamination can significantly affect deposit formation.

Static-Reactor Deposits

Typical results of atomic concentration-depth profiles are shown in Fig. 27 and Fig. 28 for static reactor Runs 63 and 64. The deposits were produced at 625 F at (603 K) over a period of 2 1/2 hours. In Run 63, a new tube with new caps was used. For this run, the AES results clearly show extremely-high concentration of chlorine (up to 55 percent), qualitatively similar to the results from the flow reactor experiments. Note that the carbon atomic fraction is reduced to 15 percent, well below the 50 percent that might be considered normal. In the

next test, Run 64 (Fig. 28), in which the same tube and fittings were re-used, substantially-smaller quantities of deposit were produced. The maximum chlorine concentration has fallen to less than 25 percent. Concentrations of carbon remained the same, slightly larger amounts of oxygen were measured, and small concentrations of sulphur were found. Stated another way, the weight of chlorine was 275 μg in Run 63, but dropped to less than 10 μg in Run 64. Carbon was 90 μg in Run 63, dropping to 10 in Run 64. In both runs, the carbon fraction appears to be nearly constant with depth, while chlorine is dropping, indicating that chlorine may be less-uniformly deposited.

As described previously in this report, SEM measurements were made of the tube and fittings in an effort to determine the source of the chlorine. Although the results are not definitive, it is believed that chlorine is not furnished by the system or by the preparation of the system. It is unlikely that methylene chloride (CH_2Cl_2), which was used for initial cleaning in many experiments, was the source of the chlorine found in the deposits. Methylene chloride is highly volatile and should evaporate completely at 40 C, its boiling point; moreover, a blank-run, AES analysis of a strip rinsed in methylene chloride showed no traces of chlorine.

Discussion

Atomic concentrations of coke have been determined in previous work, generally by using elemental analysis. In this technique, it is assumed that the material to be analyzed is made up of ash and the following elements: carbon, hydrogen, nitrogen, oxygen, and sulphur. The latter two elements are not determined separately, but the sum of these two is determined by difference. Other elements of interest may appear in the ash or as part of the difference (and are then included with oxygen or sulphur). The analyzer can be modified to obtain an estimate for the oxygen concentration (Ref. 1), but this technique probably provides a low estimate. Typical results of elemental analysis of coke by other workers (Refs. 5, 6) are shown in Table 4. The range in concentration for individual atoms is not unlike the wide range observed for the tests reported in this work. Relative to previous work, three items characteristics of this present study are notable. These are:

1. The range in the concentration of carbon atoms is very wide, i.e. from approximately 10 to 95 percent.

2. Chlorine was present for many of these runs, often in very high concentrations.

3. For one run, the sulphur concentration was extremely high (> 50 percent).

Although it is entirely speculative, it may be postulated that halogens were actually present in the ash or difference fractions listed in Table 5; only a direct measurement could establish whether this is true.

The ease with which chlorine or fluorine may contaminate a fuel system should not be underestimated. Halogens are contained in many standard solvents such as Freon and trichloroethylene. Traces of these compounds may contaminate the fuel or remain on surfaces prior to use. Acid (HCl) cleaning of steels can also leave traces of chlorine on the metal surfaces. Salts from the environment may contribute chlorine. Finally, fuels processed from coals or shale oil may contain chlorine due to relatively-high concentrations of chlorine in the raw feedstock; concentrations of chlorine in coal very substantially, from approximately 0.01 percent to 0.5 percent. Thus, chlorine impurities may contribute to the poor thermal stability characteristics of coal-derived fuels.

Since halogens generally form strongly-polar compounds, the conclusion that halogen impurities enhance deposit formation is in agreement with other work on the effects of polar compounds. In Ref. 7, it was shown that deposit formation was reduced substantially by removal of the polar fraction of the fuel prior to treatment. It was concluded in Ref. 6 that nitrogen, sulphur, and oxygen concentrate in the deposits and, since these atoms generally form polar organic compounds, deposits are primarily made up of polar compounds. Their relative insolubility in nearly-nonpolar hydrocarbons leads to deposit formation.

Evidence for the presence of chlorine has also been sought elsewhere by other workers. In the present study, chlorine has been detected in deposits from both the static and flow reactor tests using AES and SIMS analysis techniques. In the static reactor tests, the quantity of chlorine in the deposit correlates directly with the amount of deposit. Cleaning in a 1/1 mixture of ammonia and hydrogen peroxide, which would be expected to remove chlorine, almost totally inhibits formation of deposits, even after treating the fuel one hour at 625 F (603 K) under a blanket of air. This clearly demonstrates that chlorine (or halogens, in general) strongly influences the formation of deposits. The sources of the halogens are, at this time, uncertain and, at least in the case of the present experiments, are variable. Possible sources include solvents such as trichloroethylene or Freons, salts from handling, and remnants from acid cleaning.

Clearly, there are other poorly-understood chemical and/or physical parameters that are important to deposit formation. The difficulty of obtaining experimental repeatability and the variations between this and other studies demonstrate this fact. An extreme yet very clear example of this problem is the substantial difference in chemical composition and total weight observed on adjacent brass and stainless steel half-discs in the same run.

In summary, these chemical analyses have demonstrated the following characteristics of deposit formation.

1. Halogens play an important role in the chemical character and the total deposit weight.

2. The source of halogenated compounds (or other impurities) is not clear, but it may be either liquid or surface residue.

3. The nature of the surface on which the deposit is collected (perhaps including local surface impurities) can significantly affect the weight of the deposit and the chemical nature of the deposit.

REFERENCES

1. Vranos, A. and P. J. Marteney: Experimental Study of the Stability of Aircraft Fuels at Elevated Temperatures, NASA CR 165165, Dec. 1980.

2. Schlichting, H.: Boundary-Layer Theory, Sixth Edition, McGraw Hill, 1968.

3. Roback, R., E. J. Szetela, and L. J. Spadacinni: Deposit Formation in Hydrocarbon Rocket Fuels, NASA CR 165405, Aug. 1981.

4. Culmo, R.: "Microdetermination of Oxygen in Organic Compounds with an Automatic Elemental Analyzer," Mikrochimica Acta (Wien), 4, 811-815 (1968).

5. Hazlett, R. N. and J. M. Hall: "Jet Aircraft Fuel System Deposits," presented at American Chemical Society Meeting, Atlanta, GA, March 29-April 3, 1981.

6. Nixon, A. C.: "Autoxidation and Antioxidants of Petroleum," Chapter 17 in "Autoxidation and Antioxidants," Ed by W. O. Lundberg, John Wiley, New York (1962).

7. Worstell, J. H., S. R. Daniel, and G. Frauenhoff: "Deposit Formation in Liquid Fuels, 3. The Effect of Selected Nitrogen Compounds on Diesel Fuel," Fuel, 60, 485-487 (1981).

8. Goodman, H., R. Bradley, and T. Sickles: High Temperatures Hydrocarbon Fuels Research in an Advanced Aircraft Fuel System Simulator on Fuel AFFB-8-67, North American Aviation Technical Report AFAPL-TR-67-116, Sept. 1967.

TABLE 1

TABULATED TEST DATA

A. Regular Diesel Fuel-stainless steel discs except as indicated

Run	$T_{wall,F}$	Time,hr	Flow,gph	Coking Rate, $\mu g/cm^2$-hr at Disc No. 1	2	3	4	Av	Note
1	300	4	2.0	(—)	(—)	0.90	(—)	(.22)	
1R	300	4	2.0	(—)	0.26	0.80	0.71	0.59	
2	300	8	2.0	(—)	2.37	(—)	0.05	(0.65)	
3	300	4	5.0	(—)	(—)	1.73	(—)	(0.43)	
4	400	3	6.0	2.96	6.79	0.86	1.73	3.09	
5	300	4	12.0	(—)	0.90	(—)	(—)	(0.19)	
6	500	3	2.0	2.88	6.00	5.08	0.58	3.63	
7	625	3	0.75	100.47	39.80	30.86	27.96	49.77	
8	625	3	3.0	47.50	53.70	28.66	20.01	37.47	
9	500	3	0.75	5.40	7.45	5.72	2.05	5.15	
10	500	3	4.0	2.64	4.84	3.74	1.10	3.11	
11	500	3	6.0	0.46	2.08	2.65	0.23	1.37	
12	625	3	15.0	11.01	17.70	22.28	28.83	19.96	
14A1	500	3	2.0	31.20	22.30	17.40	16.20	21.75	
15A1	500	3	4.0	15.99	4.79	1.09	2.72	6.15	
16A1	500	3	6.0	11.13	7.33	7.81	9.18	8.86	
17A1	300	3	0.75	0.77	1.64	1.97	3.28	1.91	
19A1	500	3	0.75	8.63	15.48	8.18	4.37	9.17	
21	300	3	0.75	1.17	2.22	2.45	—	1.95	
22	625	3	2.0	75.48	65.18	48.39	28.10	54.24	
24Br	500	3	2.0	40.60	40.13	37.45	29.17	36.84	
25Br	500	3	0.75	40.60	45.99	45.76	30.17	40.59	
26	500	3	2.0	5.64	7.74	7.74	12.16	8.32	Q
27A1	500	3	2.0	7.58	3.15	0.82	(15.28)	3.85	Q
28	500	3	0.75	7.87	7.35	(0.47)	(—)	7.41	Q
29Br	625	3	0.75	(46.67)	44.10	28.00	8.87	31.91	Q
30	625	3	0.75	81.65	48.00	22.05	13.80	41.40	Q
31	625	3	2.0	40.37	42.23	28.12	16.32	31.76	Q
32A1	500	3	0.75	3.58	8.40	3.83	1.85	4.41	Q
35	625	3	2.5	12.27	16.69	16.69	8.62	13.57	I
38	625	1 2/3	1.35	13.60	16.80	4.20	7.80	10.60	I
39	625	1	2.25	33.95	23.80	22.30	9.45	23.63	
41	625	3	0.75	9.68	6.88	10.27	3.62	7.61	BP
42	625	3	0.75	7.00	6.88	5.02	1.75	5.14	P
44	625	3	0.75	(lost)	19.82	10.33	0.70	10.28	D,P

TABLE 1 (Cont'd)

TABULATED TEST DATA

B. Premium Diesel Fuel-stainless steel discs except as noted

Run	$T_{wall,F}$	Time,hr	Flow,gph	Coking Rate, $\mu g/cm^2$-hr at Disc No. 1	2	3	4	Av	Note
101	625	3	2.25	79.06	33.21	13.96	19.48	36.43	
102	625	3	0.75	103.25	39.67	16.33	9.33	42.14	
103	625	3	0.75	22.58	11.38	9.63	14.00	14.40	
105	625	8	0.75	177.19	81.03	79.17	93.32	107.68	
106	625	5	0.75	67.69	59.36	21.35	11.34	39.94	
107	500	3	0.75	9.22	10.27	12.14	9.92	10.39	
112	500	3	0.75	3.50	6.07	3.85	1.52	3.73	
114	625	3	0.75	23.33	29.17	10.27	5.02	16.95	
115	625	3	0.75	9.92	41.42	15.17	11.90	19.60	
116Tabs	625	3	0.75	110.02	(69.42)	66.14	56.97	75.64	
117	625	3	2.25	56.60	31.28	23.11	24.16	33.79	
120	625	3	0.75	69.02	36.18	24.86	15.17	36.33	
121SS	625	3	0.75	17.03	23.34	14.00	8.87	13.81	Split
Br				88.69	74.69	103.40	57.05	81.46	Discs
125SS	625	3	0.75	63.00	42.00	18.78	16.80	25.15	
Tabs				46.14	35.23	19.54	12.02	28.23	
127SS	625	3	0.75	62.32	34.43	19.61	11.09	31.86	P
Tabs	Preheated Fuel 300 F			60.33	29.35	14.88	5.87	27.61	
130R SS	625	3	0.75	70.44	23.34	5.53	5.88	26.05	P
Tabs	Preheated Fuel 300 F			26.17	13.99	9.29	4.94	13.60	

Notes to Table:

—	Rate zero
( )	Rate uncertain
R	Repeat run
Q	Quinoline added to fuel
I	Indole added to fuel
BP	Benzoyl peroxide added to fuel
P	Fuel preheated to 300 F
D	Fuel Sparged with nitrogen

Split discs- paired halves
Tabs - discs suspended mid-channel

TABLE 2

SUMMARY OF STATIC REACTOR TESTS
(Regular Diesel Fuel, T=6031 C)

Run No.	Time (min)	Pretreatment Strip	Pretreatment Tube	Weight of Deposit (µg)	Comments
63	150	A	A	543	New tube and fittings, Auger analysis
64	150	A	A	58	Auguer analysis
65	150	A	A	65	
66	60	A	A	17	Auger analysis
67	60	A	A	329	New tube and fittings, Auger analysis
68	60	A	A	36	
69	30	A	A	63	Weight determined 3 days after test, strip not rinsed and reheated
70	30	A	A	36	
71	90	A	A	45	
72	60	A	A	6	Severe leak
74	60	A	C	782	New end caps, old tube
75	60	A,C	A,C	801	28 µl Trichloroethylene added to fuel
76	60	A	C	(-2)	
77	60	A,C	A,C,D	8	
78	60	A	A	(-5)	New tube, old caps
79	60	A	B,C	10	0.56 µl Trichloroethylene added to fuel
80	60	B,C	A,C	26	Small leak, 4 µl Trichloroethylene

A Rinsed in methylene chloride
B Rinsed in hexane/benzene mixture
C Ultrasonically cleaned in NH_4 OH/H_2O_2 solution
D Soaked in HCl

TABLE 3

COMPARISON OF OXYGEN-TO-CARBON
RATIOS (ATOM BASIS)

	O/C Ratio at 25 Å ISS	O/C Ratio at 15-35 Å AES
Run 9 (33) SS Disc	10.11 ± 0.4	0.025 ± 0.01
Run 25 (B9) Brass Disc	0.75 ± 0.2	2.2 ± 0.4
Run 19 (X21), Aluminum Disc	0.30 ± 0.1	0.045 ± 0.01

TABLE 4

ELEMENTAL ANALYSIS OF DEPOSITS
IN PREVIOUS STUDIES

	Cumulative Heat Exchanger Deposit[a]	Oxygen Bomb Deposit[a]	Engine, GE CF-6[b]	Engine, PWA TF-30[b]
carbon, %w	70.6	60.6	50.8	56.7
hydrogen, %w	4.7	4.0	2.4	3.0
nitrogen, %w	3.3	4.6	0.6	1.4
oxygen, %w	14.7	14.8	20.5	26.0
sulfur, %w	1.4	5.3	c	c
ash and unaccounted, %w	5.3	6.0	26.2	12.9

a Ref. 6
b Ref. 5
c Not reported

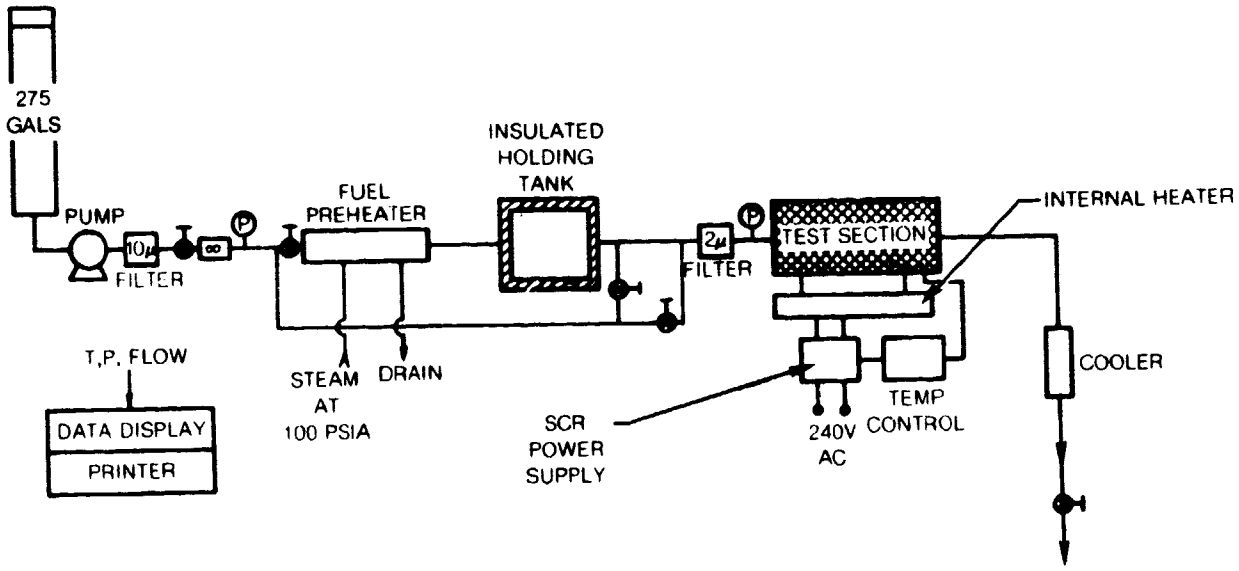

Figure 1. — Schematic Drawing of Test System

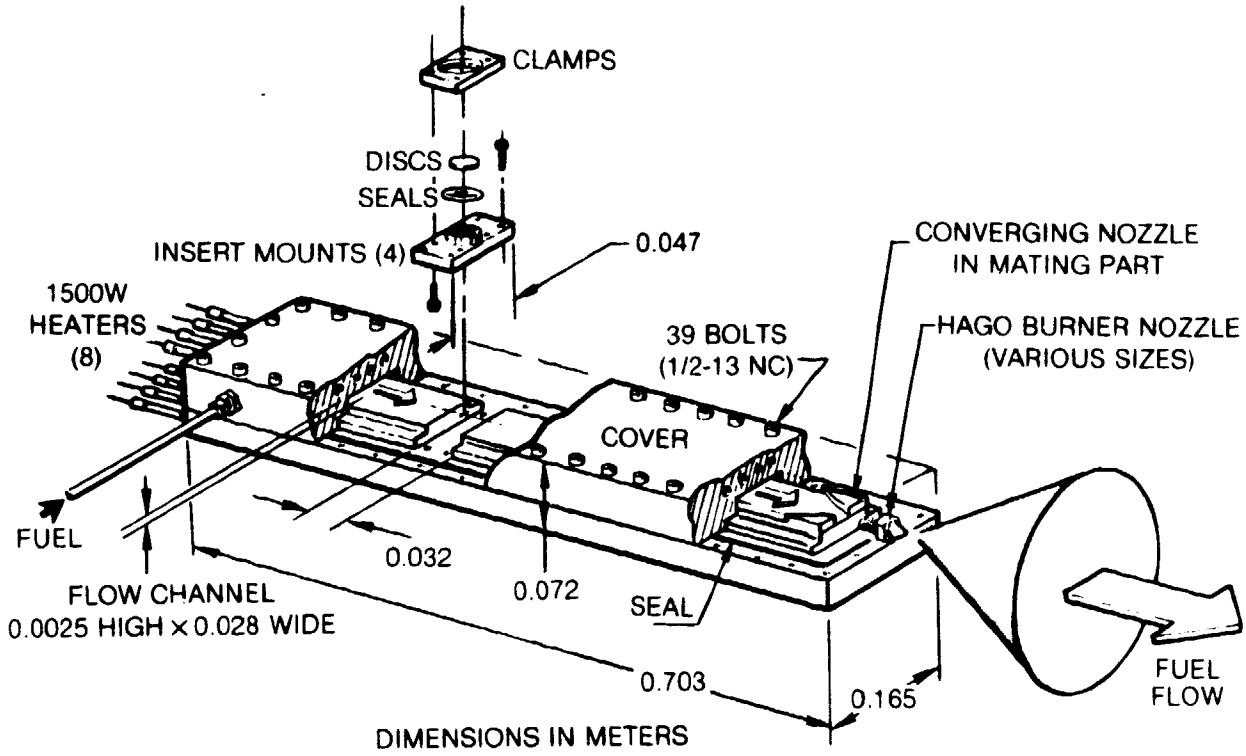

Figure 2. — Schematic Drawing of Fuel System Simulator

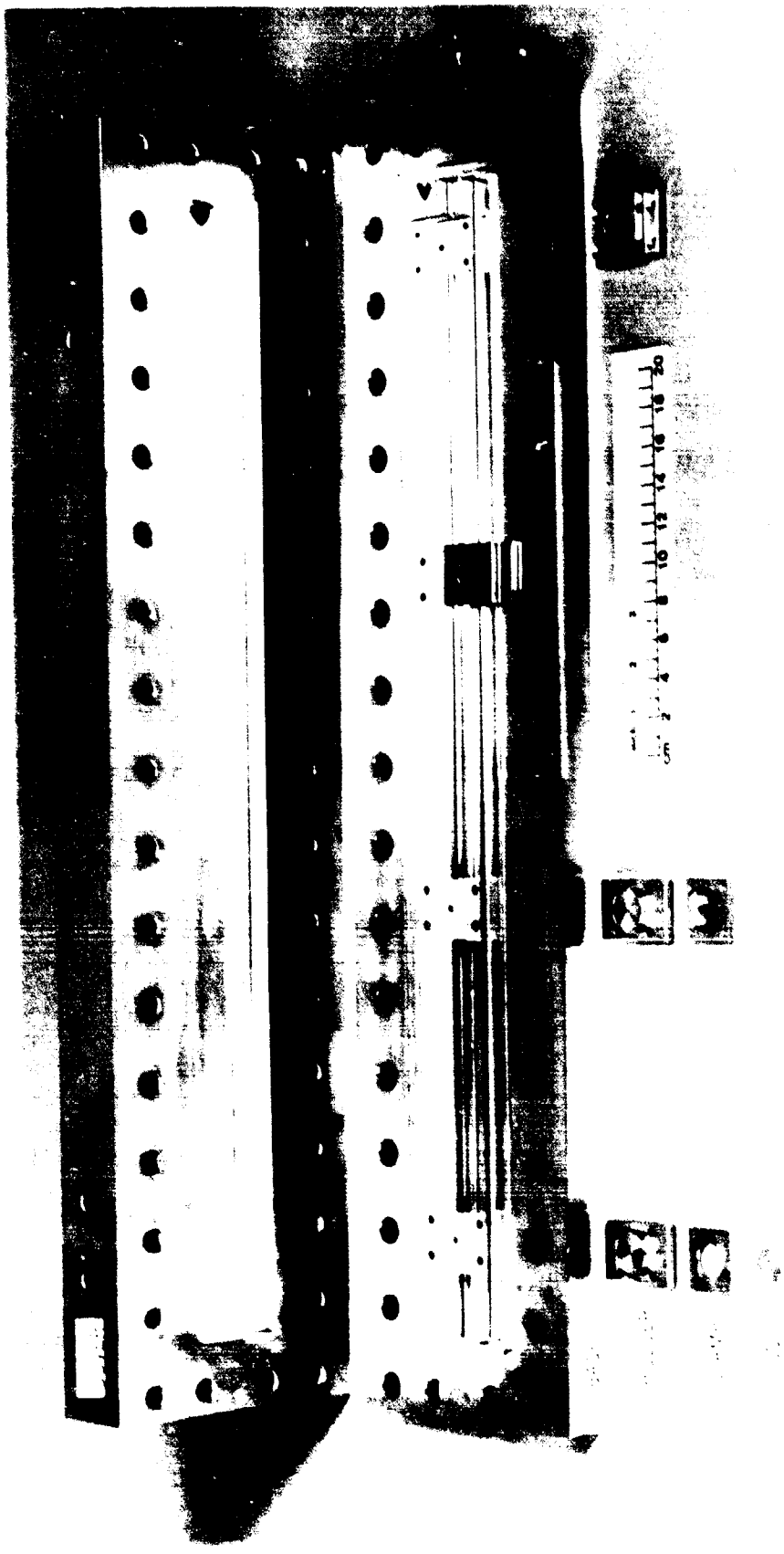

Figure 3. — Photograph of Simulator Parts

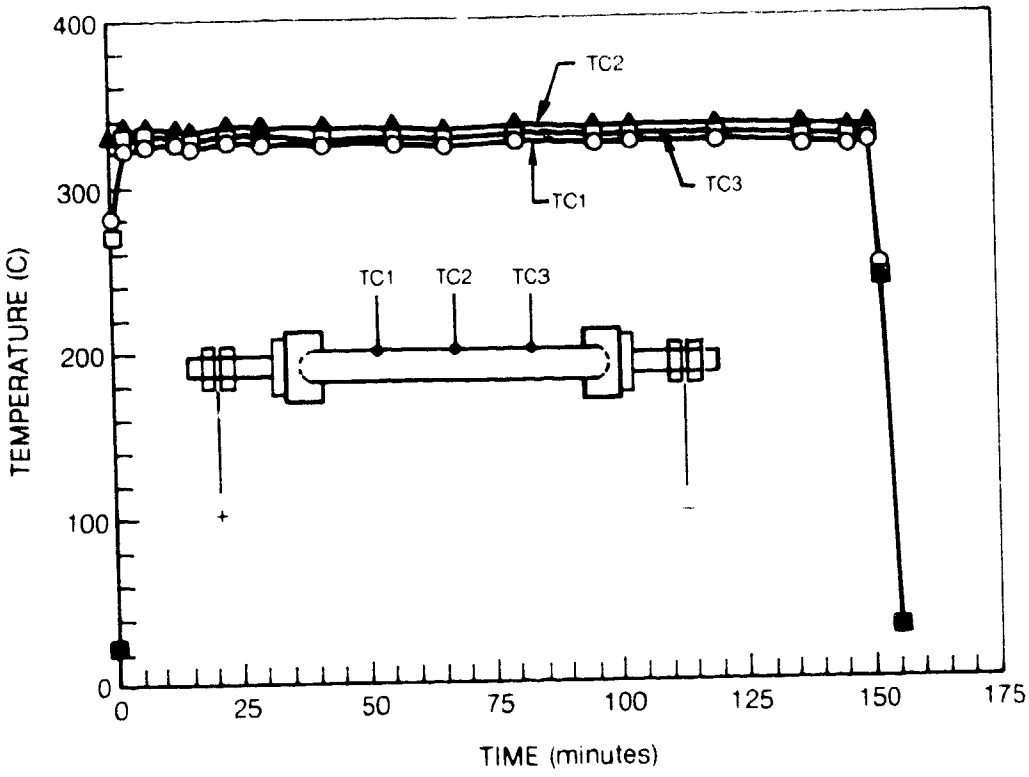

Figure 4. — Temperatures Profiles in Static Reactor

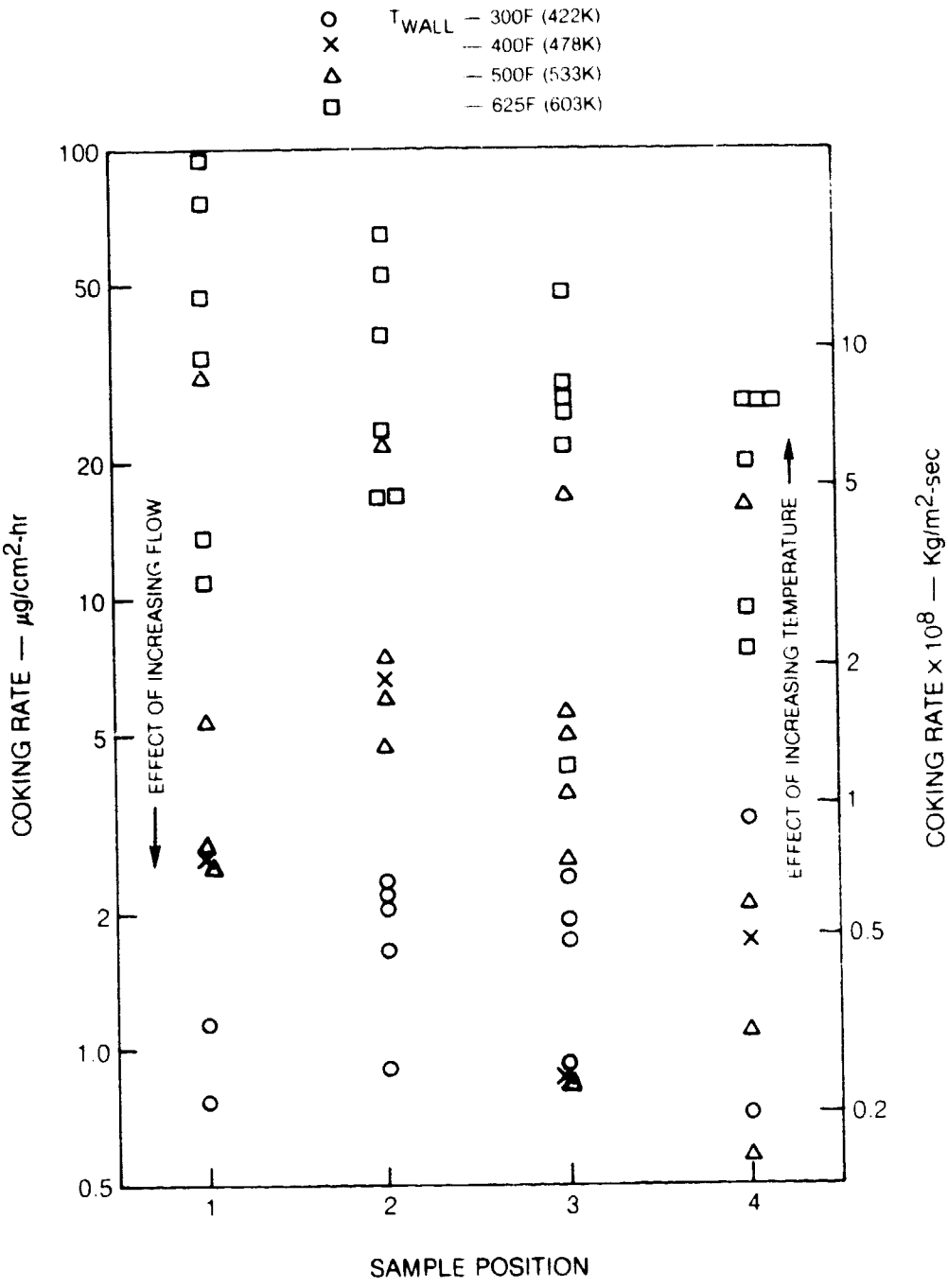

Figure 5. — Profile of Coking Rate in Regular Diesel Fuel

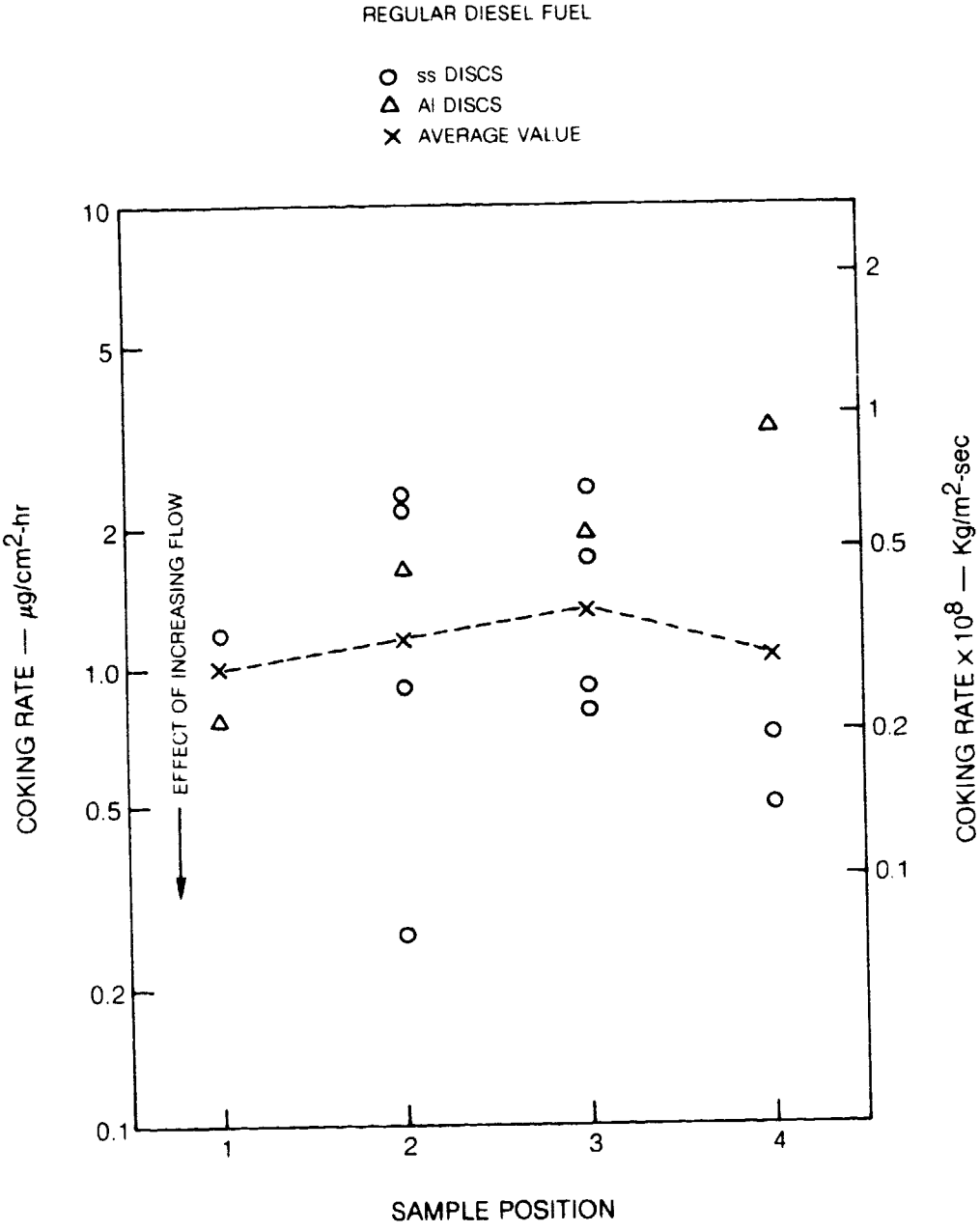

Figure 6. — Coking Profile at 300F (422K)

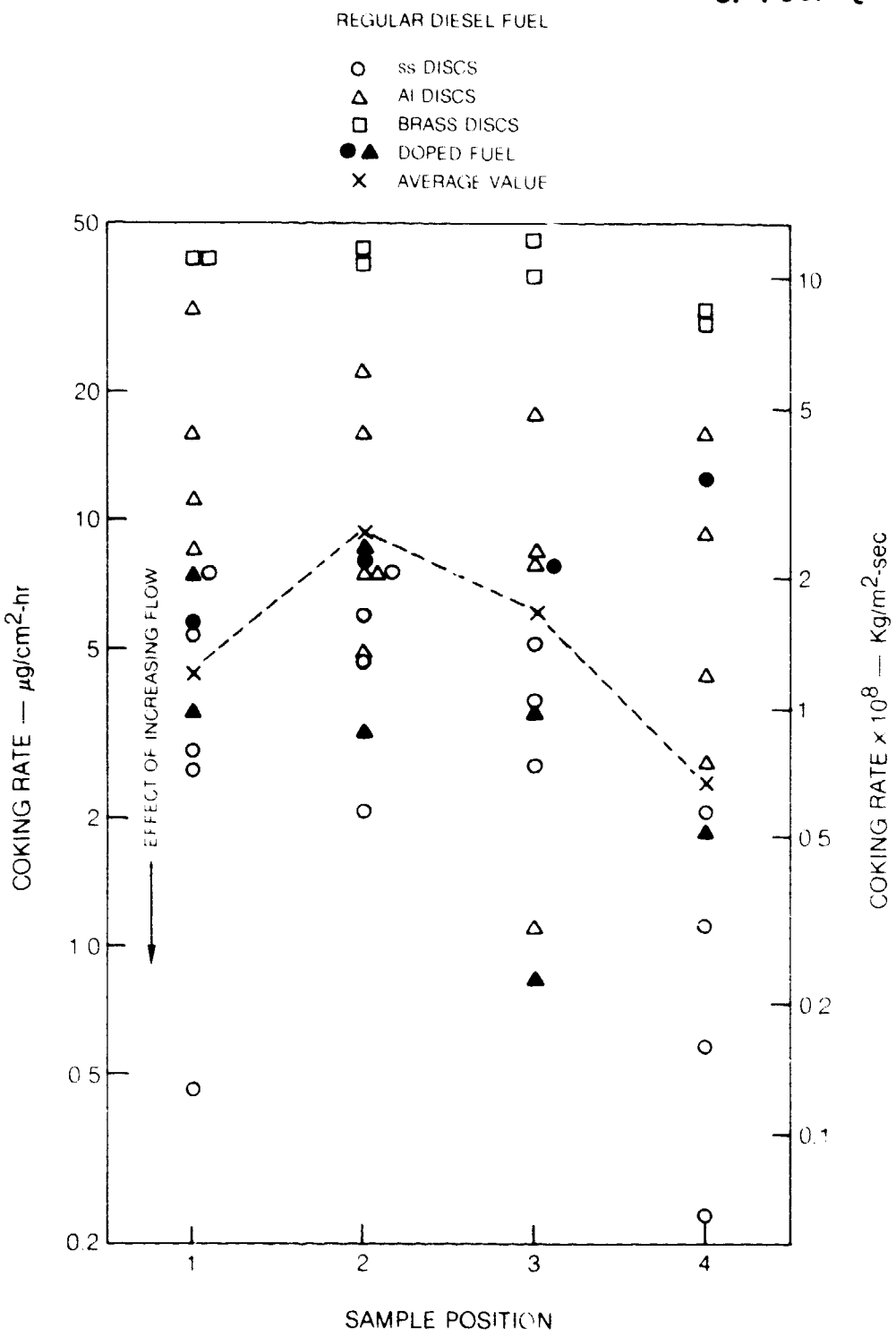

Figure 7. — Coking Profile at 500F (533K)

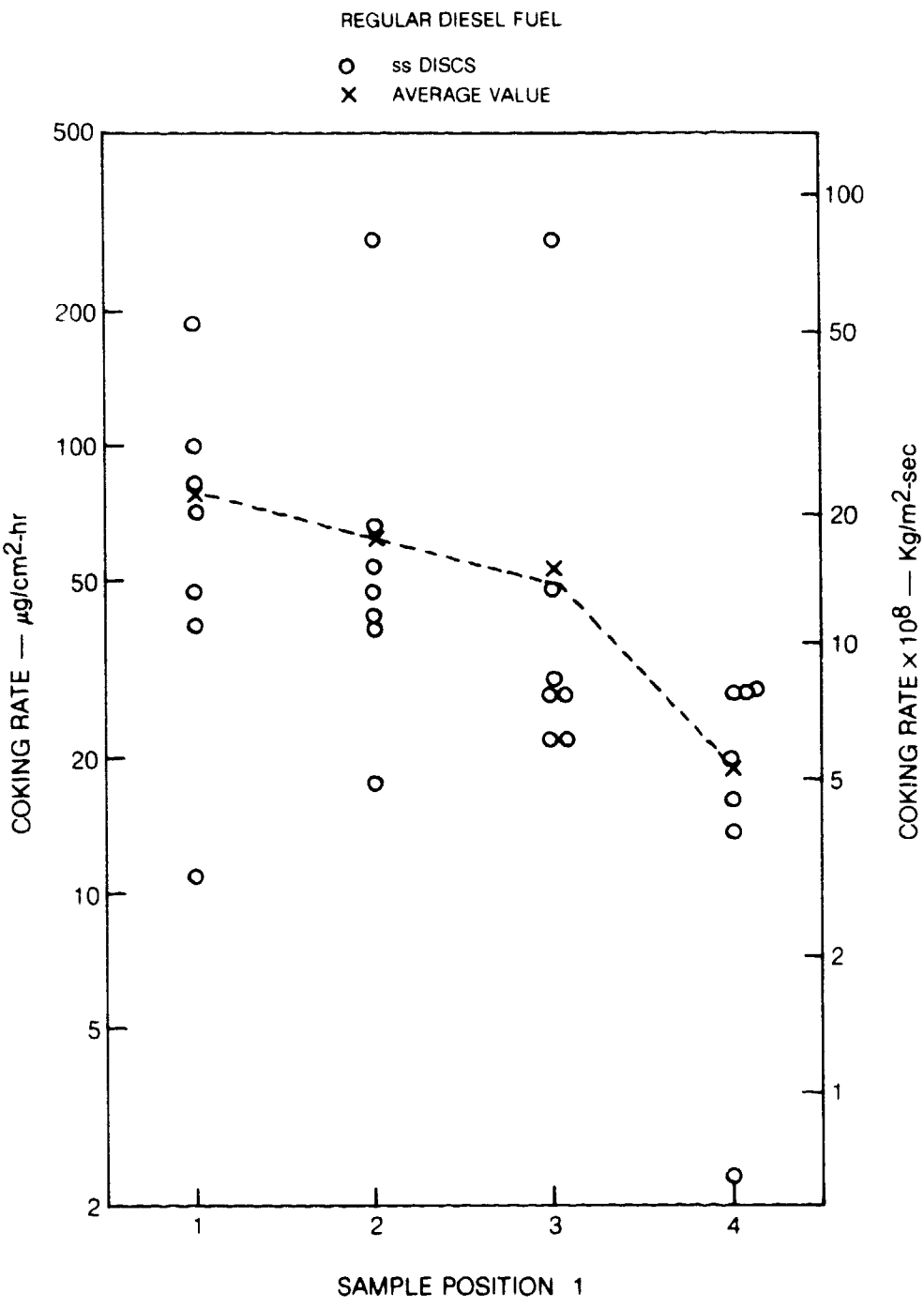

Figure 8. — Coking Profile at 625F (603K)

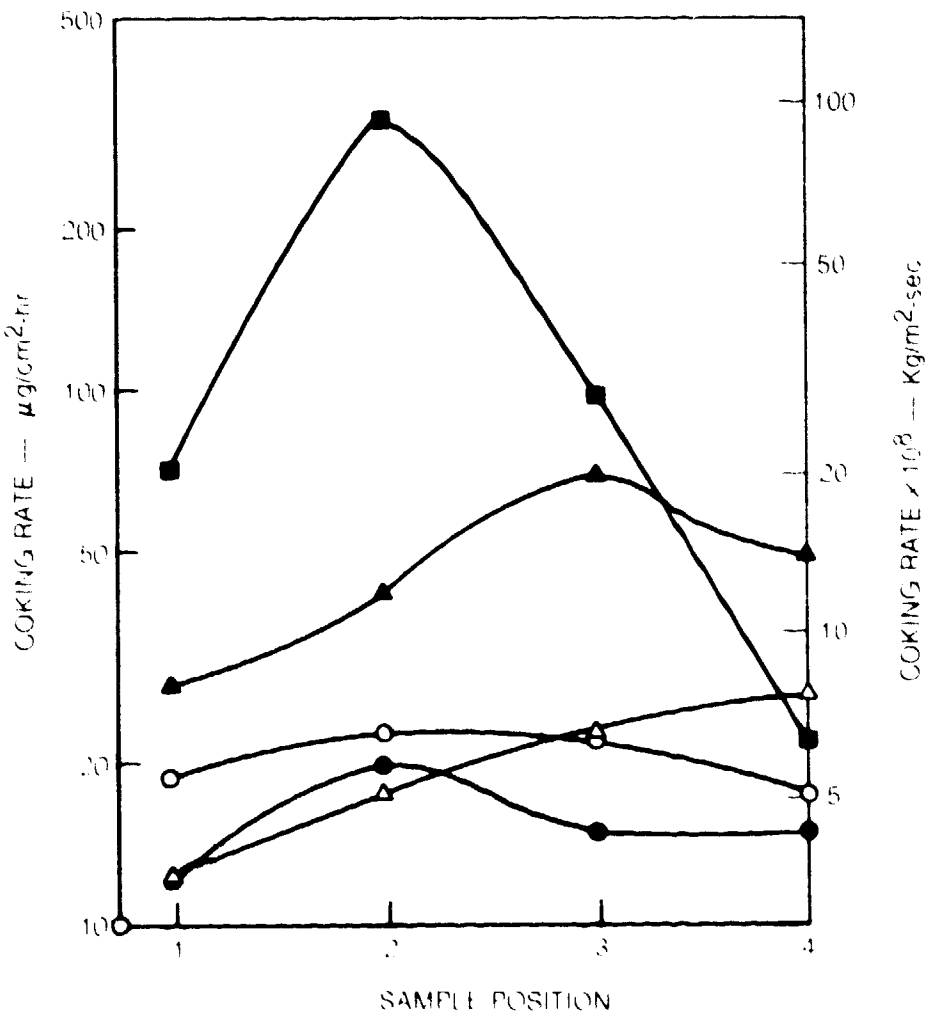

Figure 9. — Coking Rate of No. 2 Home Heating Oil vs Sample Position (From Ref. 1)

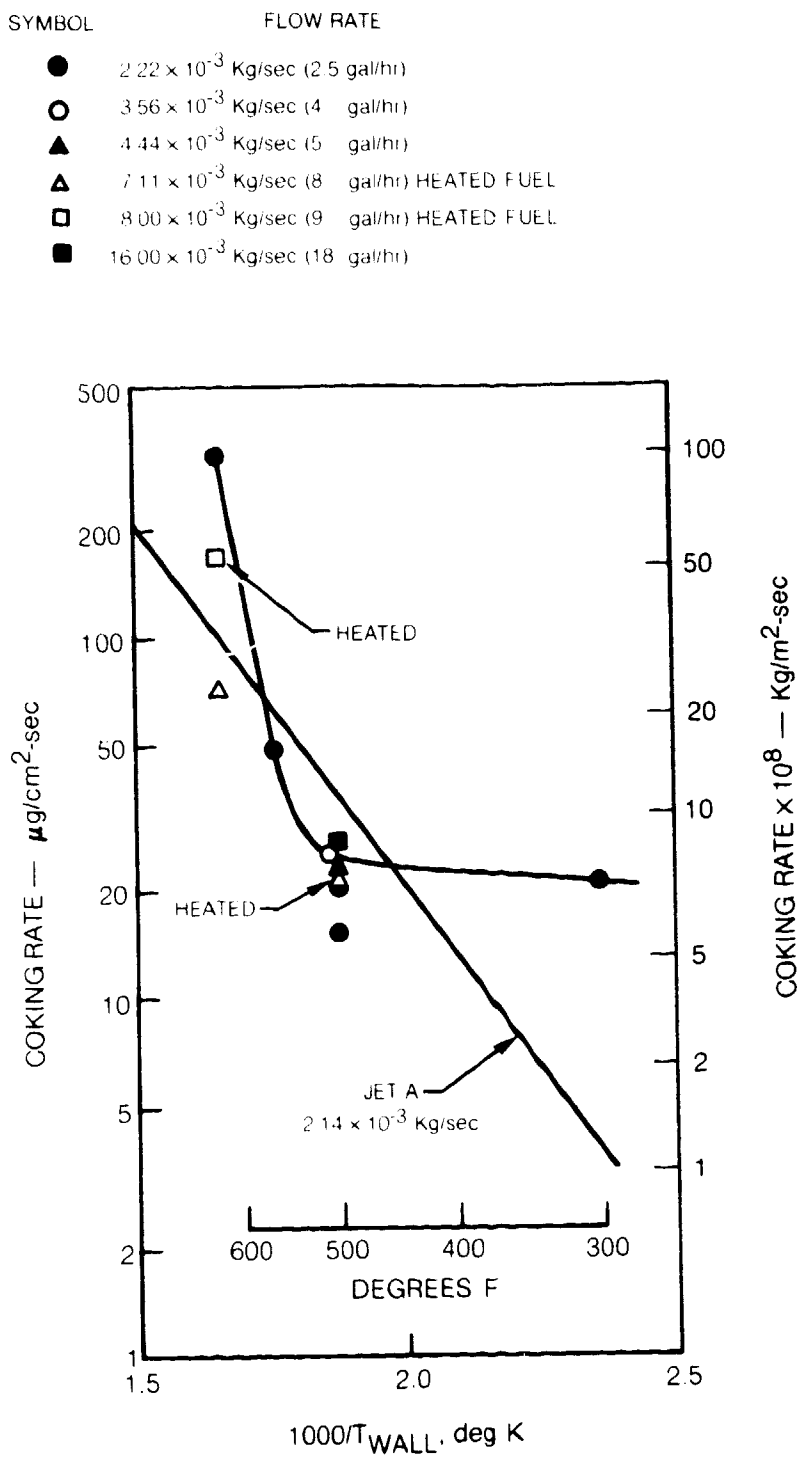

Figure 10. — Arrhenius Plot of Coking Rate in No. 2 Home Heating Oil (From Ref. 1)

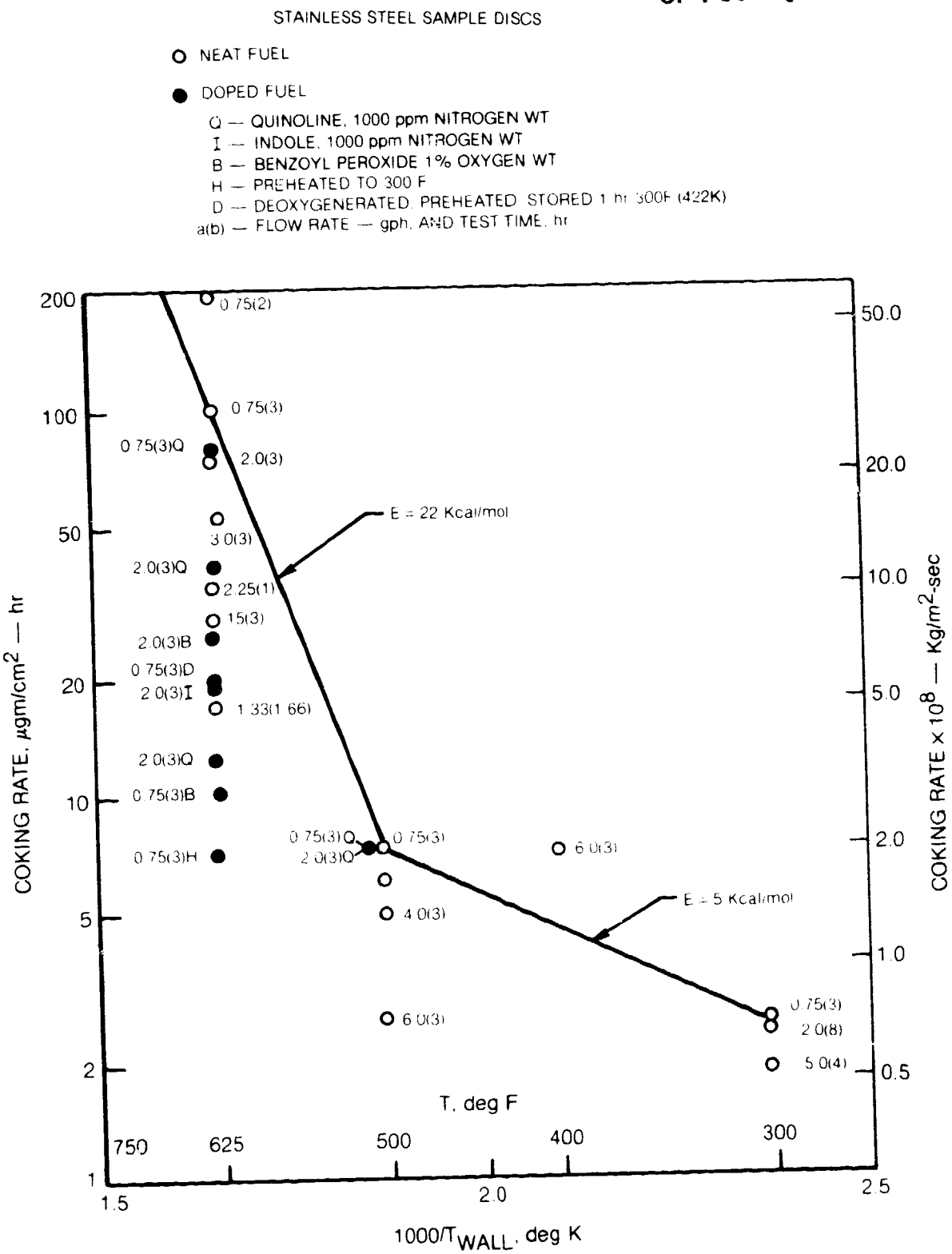

Figure 11. — Maximum Coking Rate in Regular Diesel Fuel

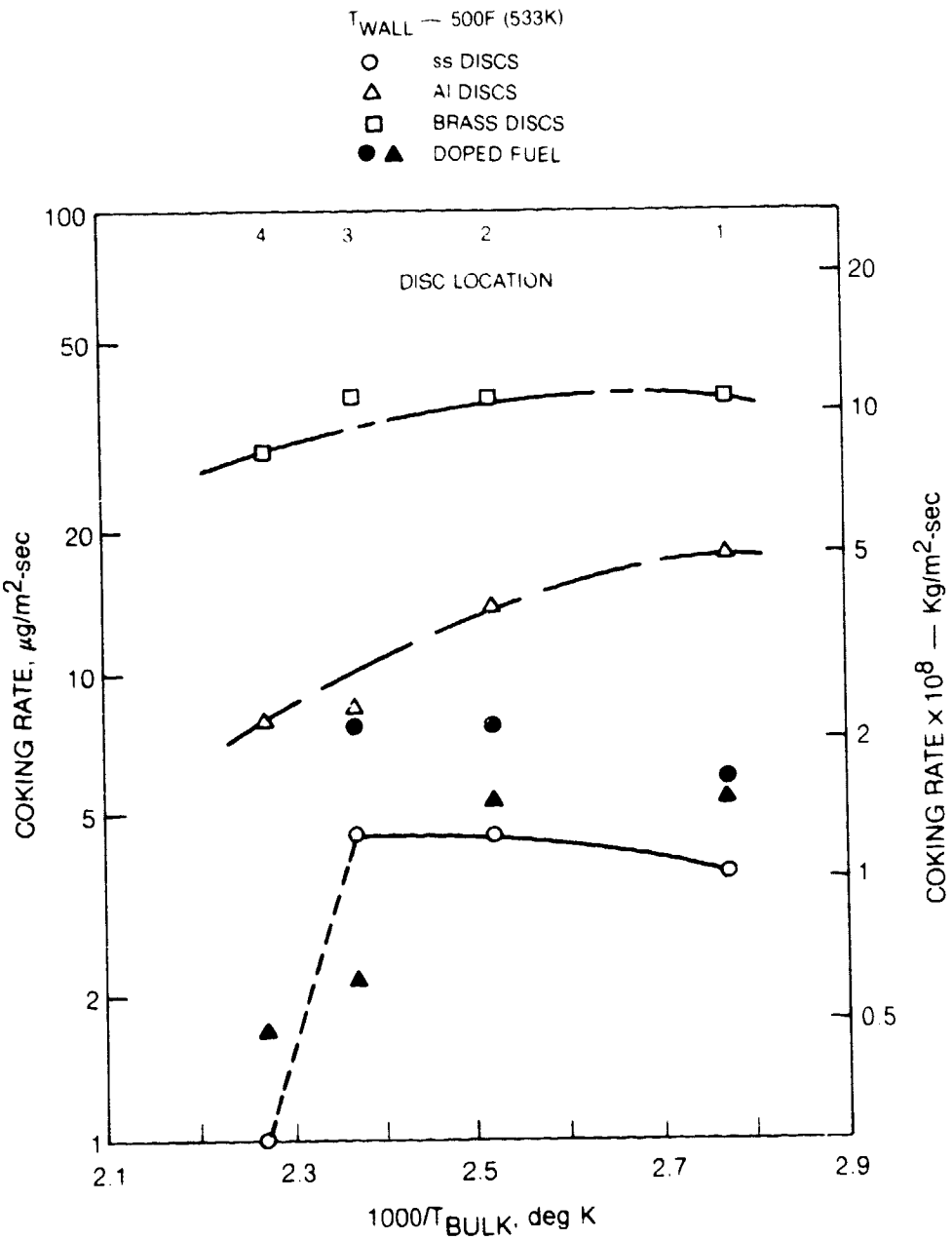

Figure 12. — Correlation of Coking Rate with Bulk Temperature

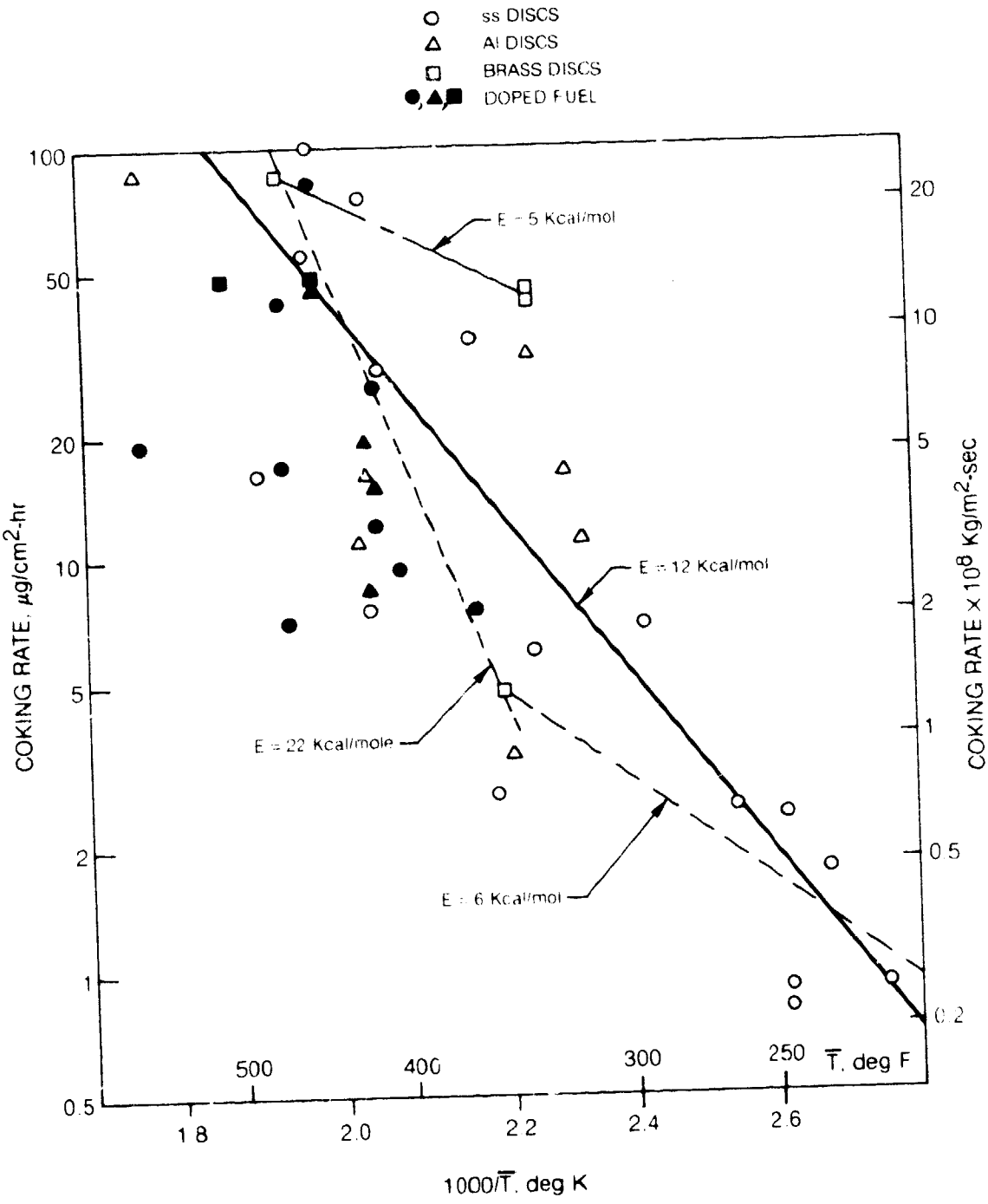

Figure 13. — Correlation of Maximum Coking Rate in Regular Diesel Fuel with Average of Wall and Fluid Temperature

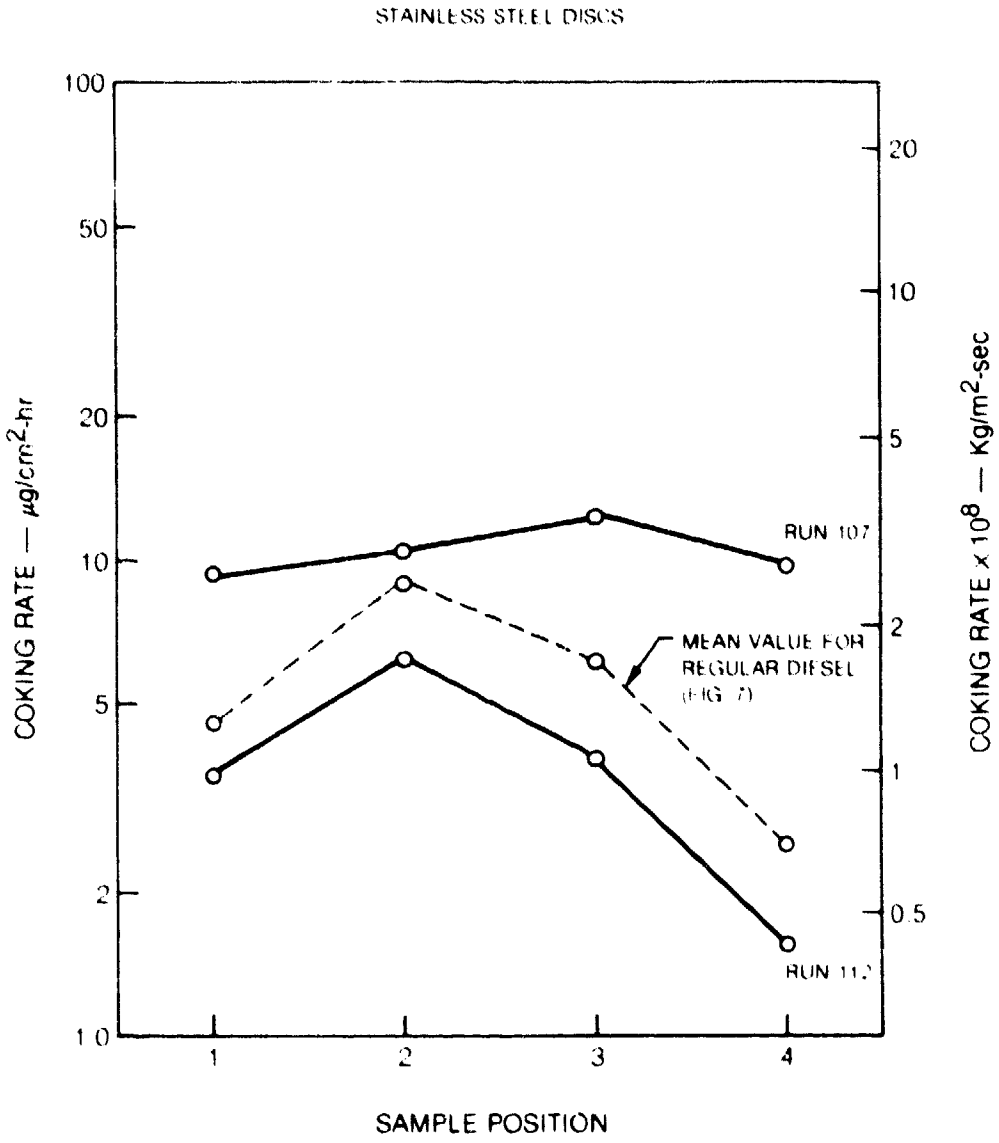

Figure 14. — Coking Rate in Premium Diesel Fuel at 500F (533K)

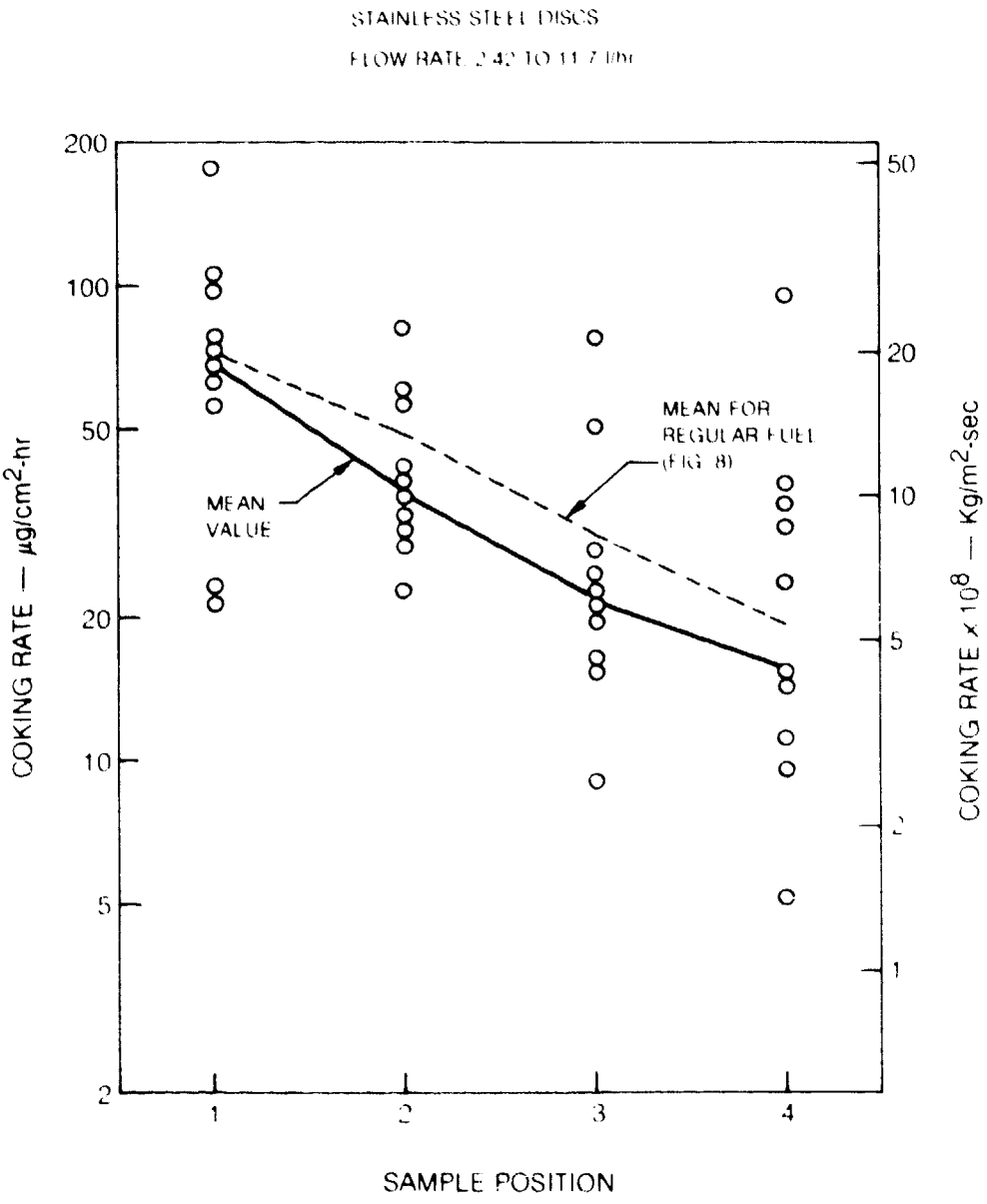

Figure 15. — Coking Rate in Premium Diesel Fuel at 625F (603K)

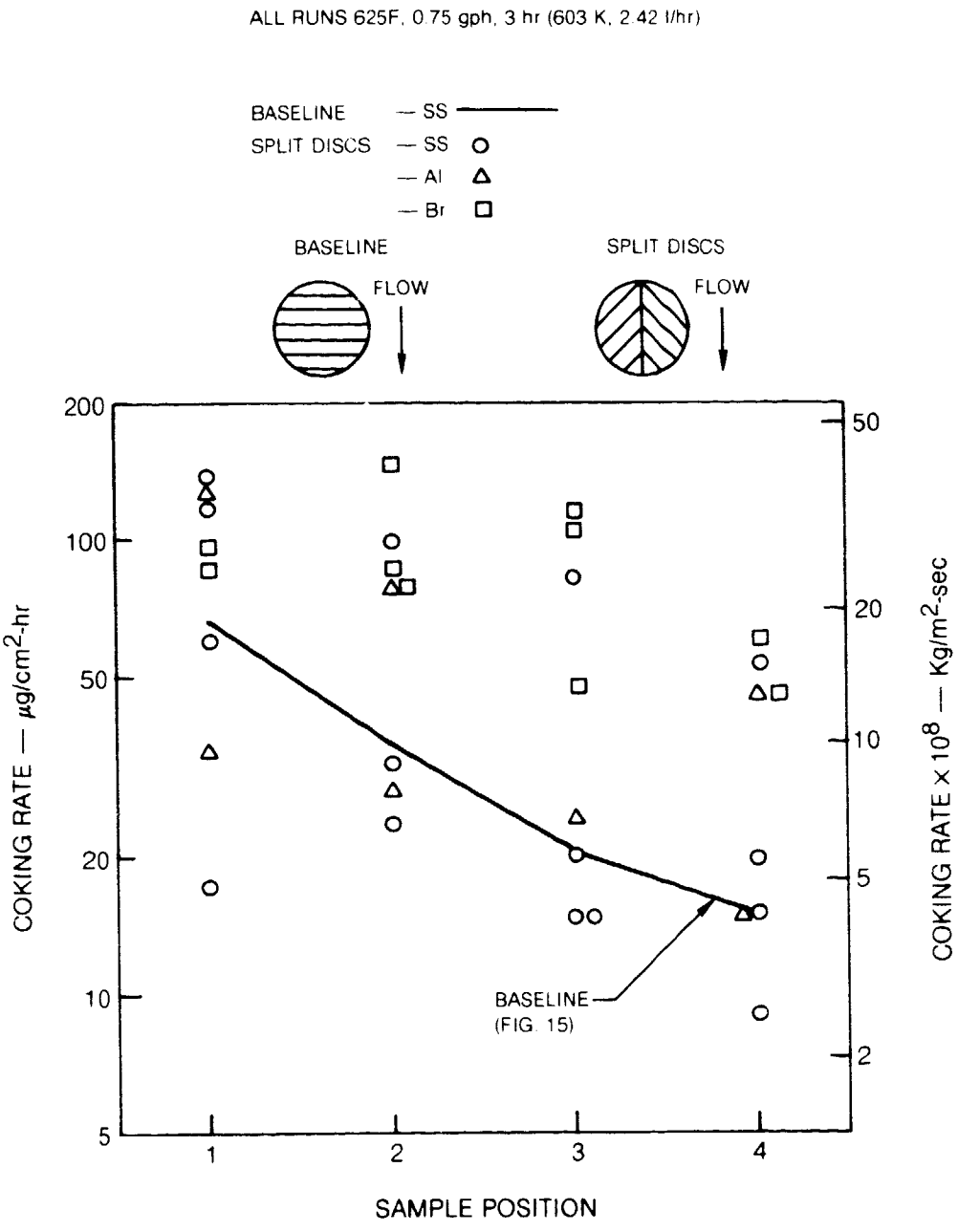

Figure 16. — Variation of Coking Rate in Premium Diesel Fuel with Disc Material or Configuration

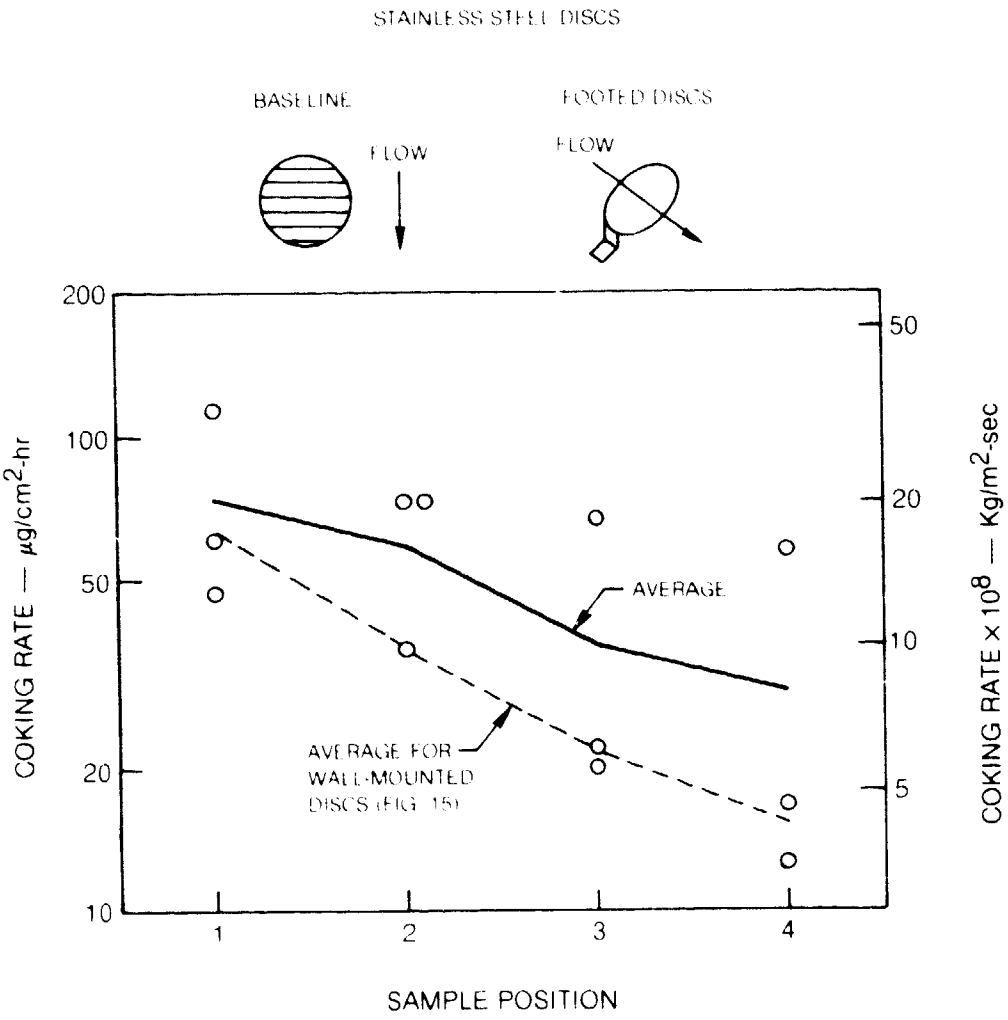

Figure 17. — Coking in Premium Diesel Fuel on Mid-Span Discs at 625F (603K)

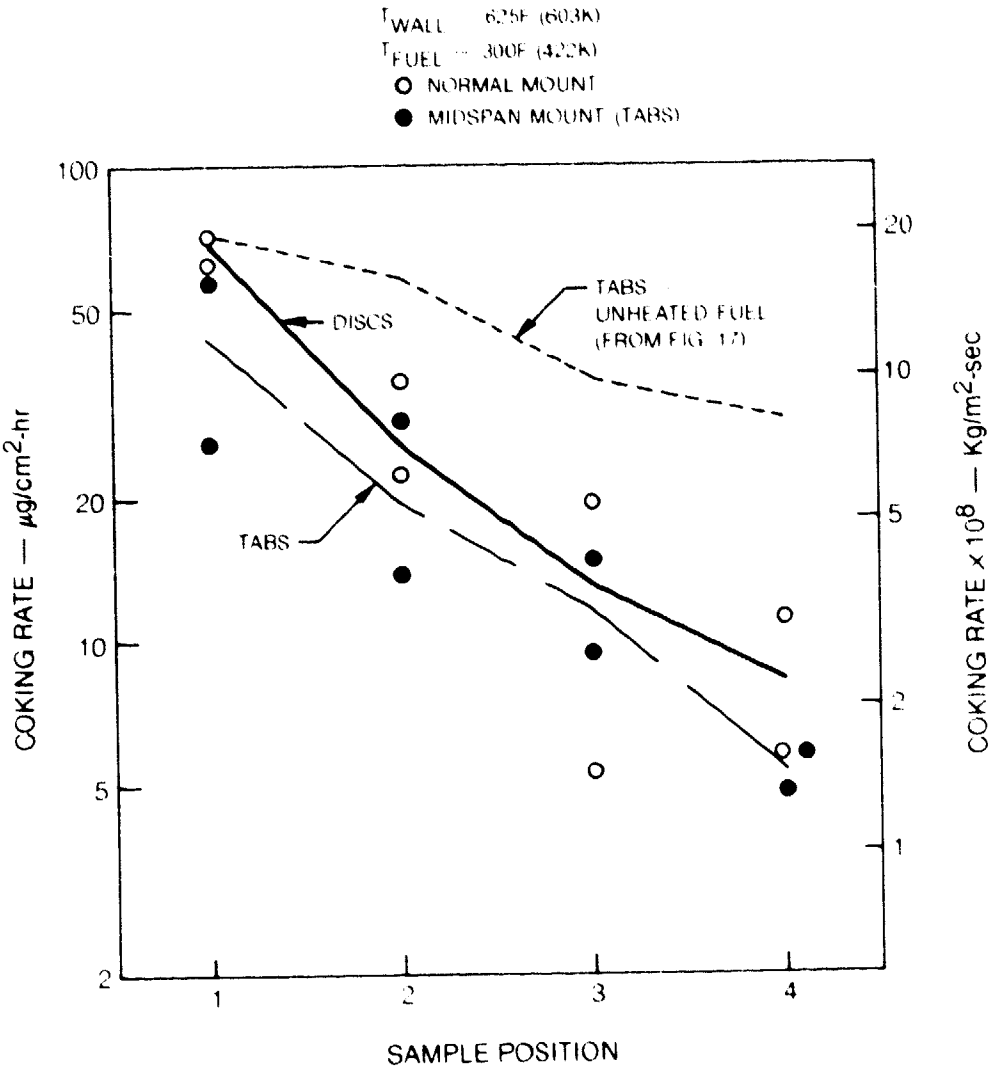

Figure 18. — Variation of Coking Rate in Preheated Premium Diesel Fuel with Disc Position

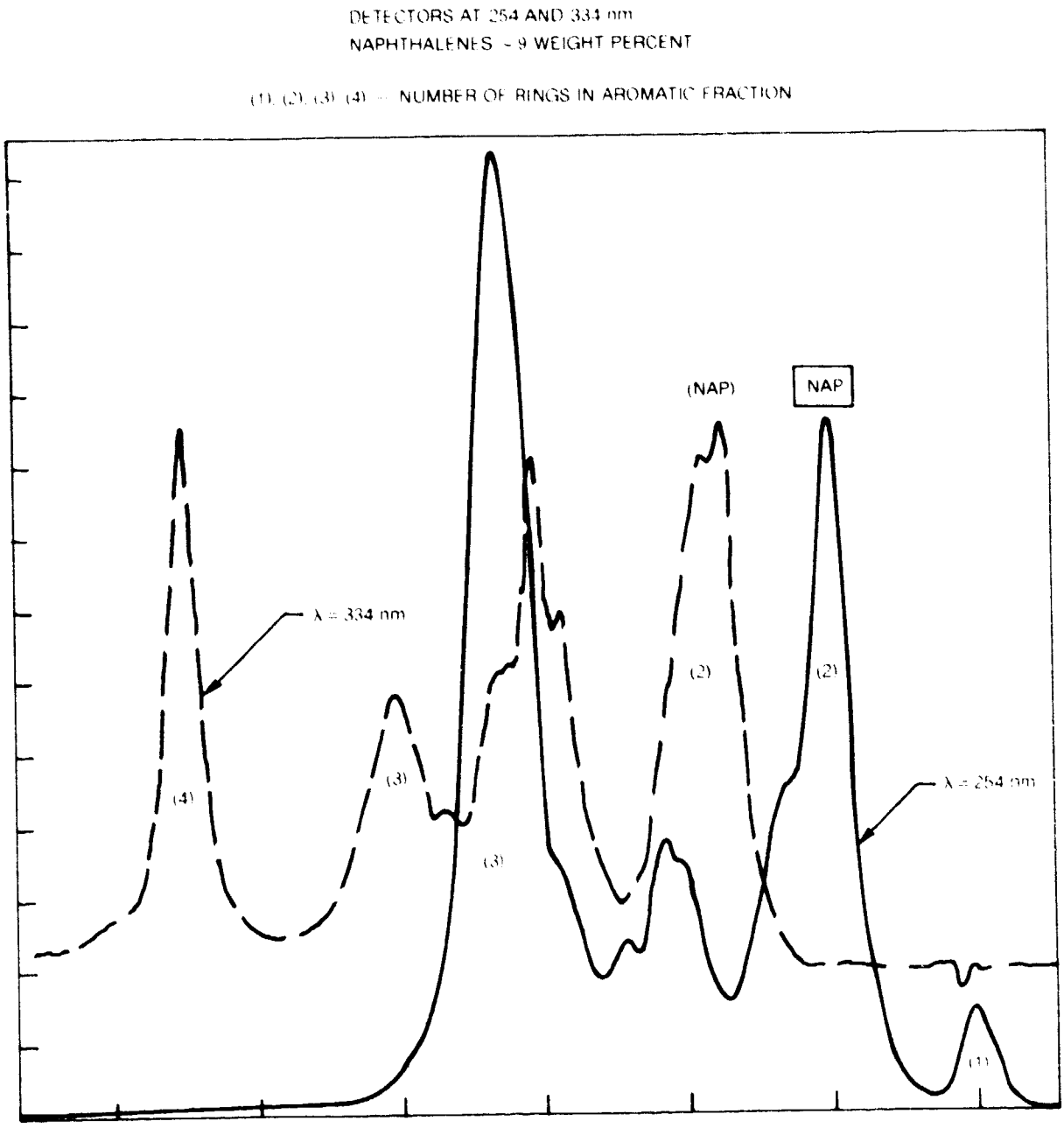

Figure 19. — Liquid Chromatogram of Regular Diesel Fuel

ORIGINAL PAGE IS
OF POOR QUALITY

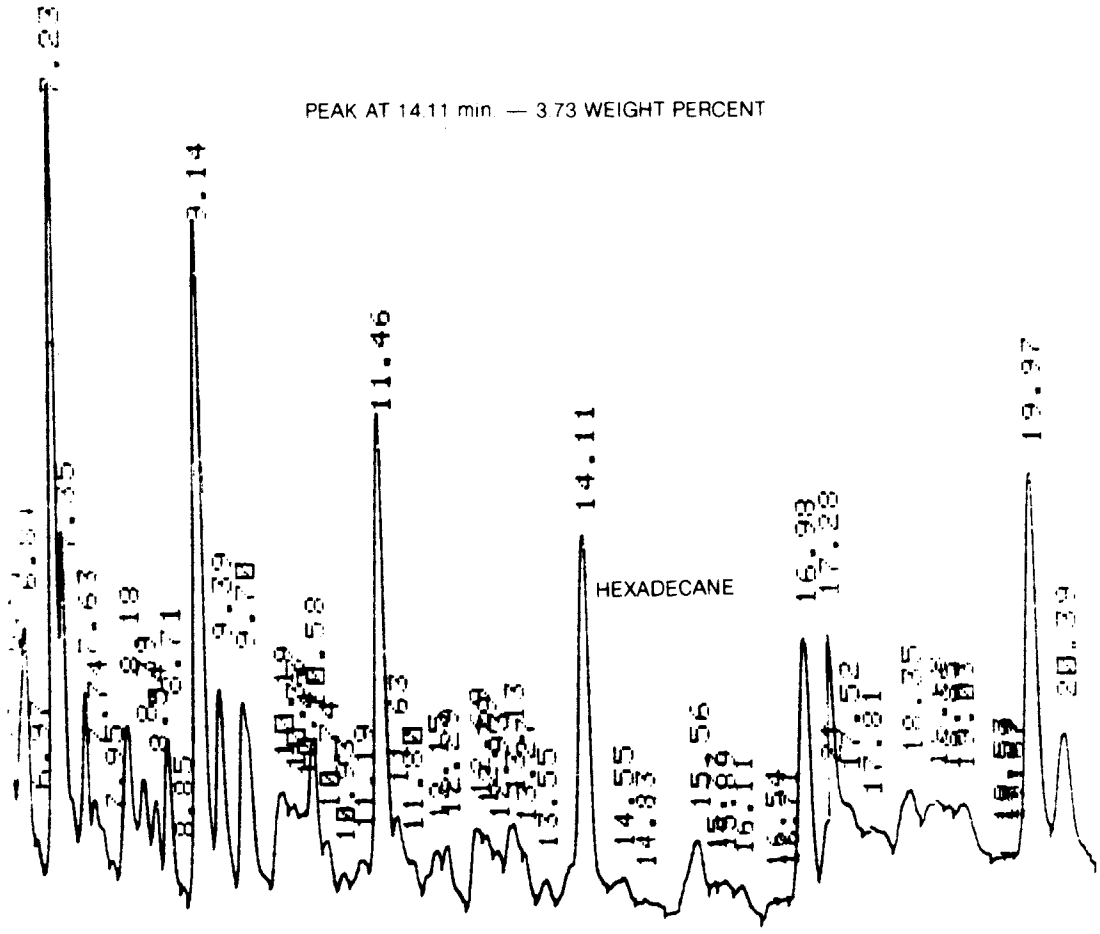

Figure 20. — CG/FID Chromatograph of Regular Diesel Fuel

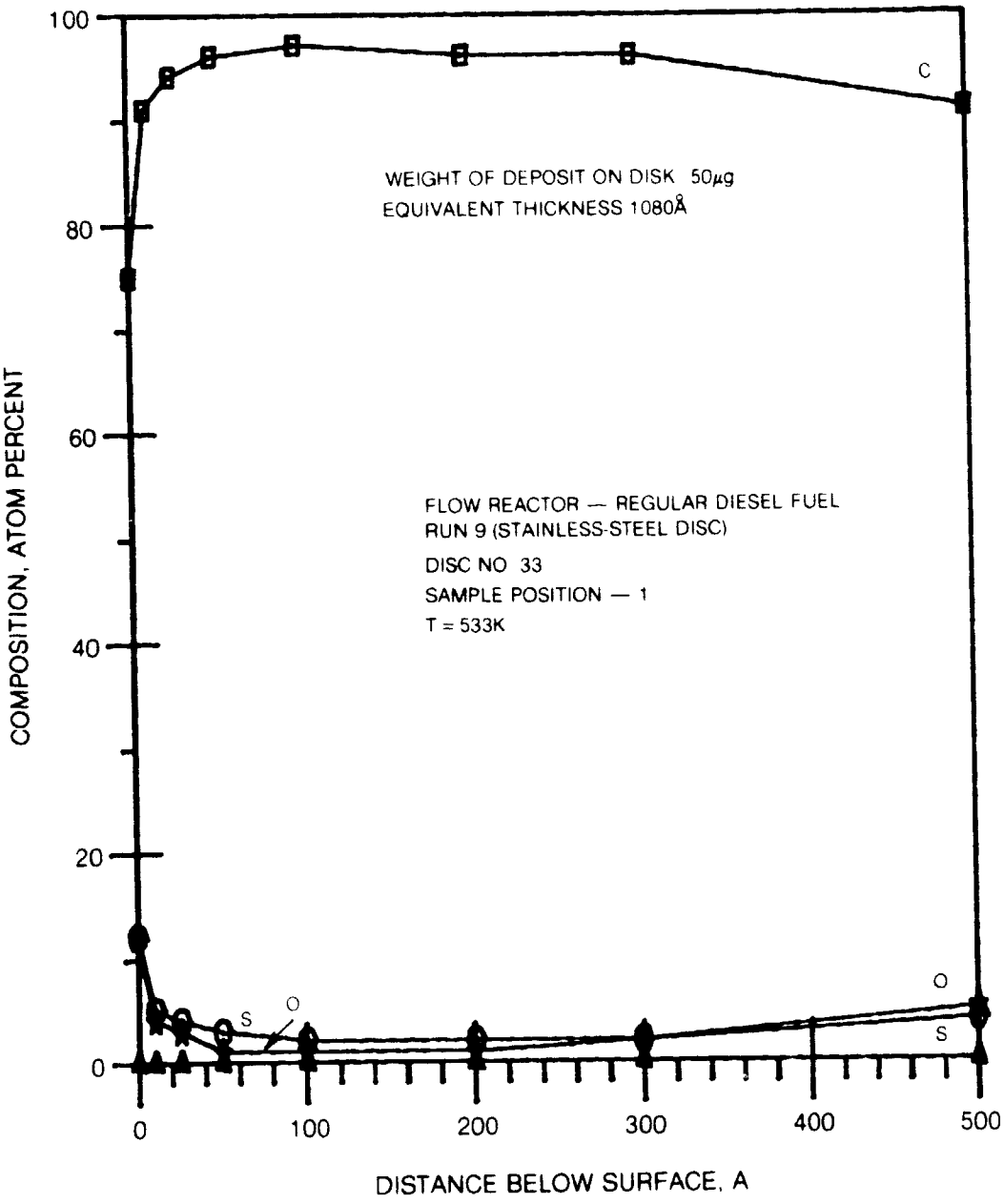

Figure 21. — AES Analysis of Deposit on Stainless Steel in Regular Diesel Fuel

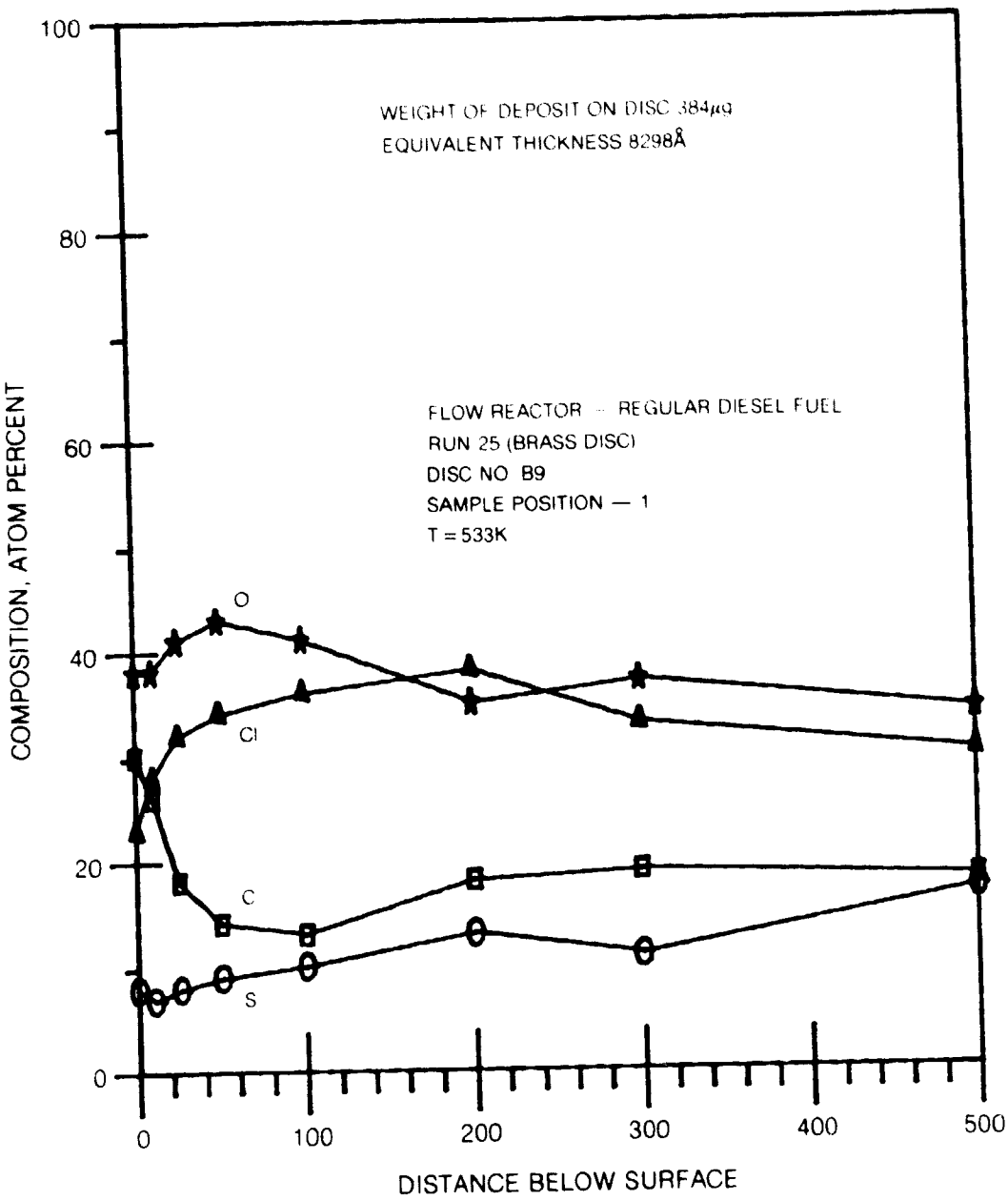

Figure 22. — AES Analysis of Deposit on Brass in Regular Diesel Fuel

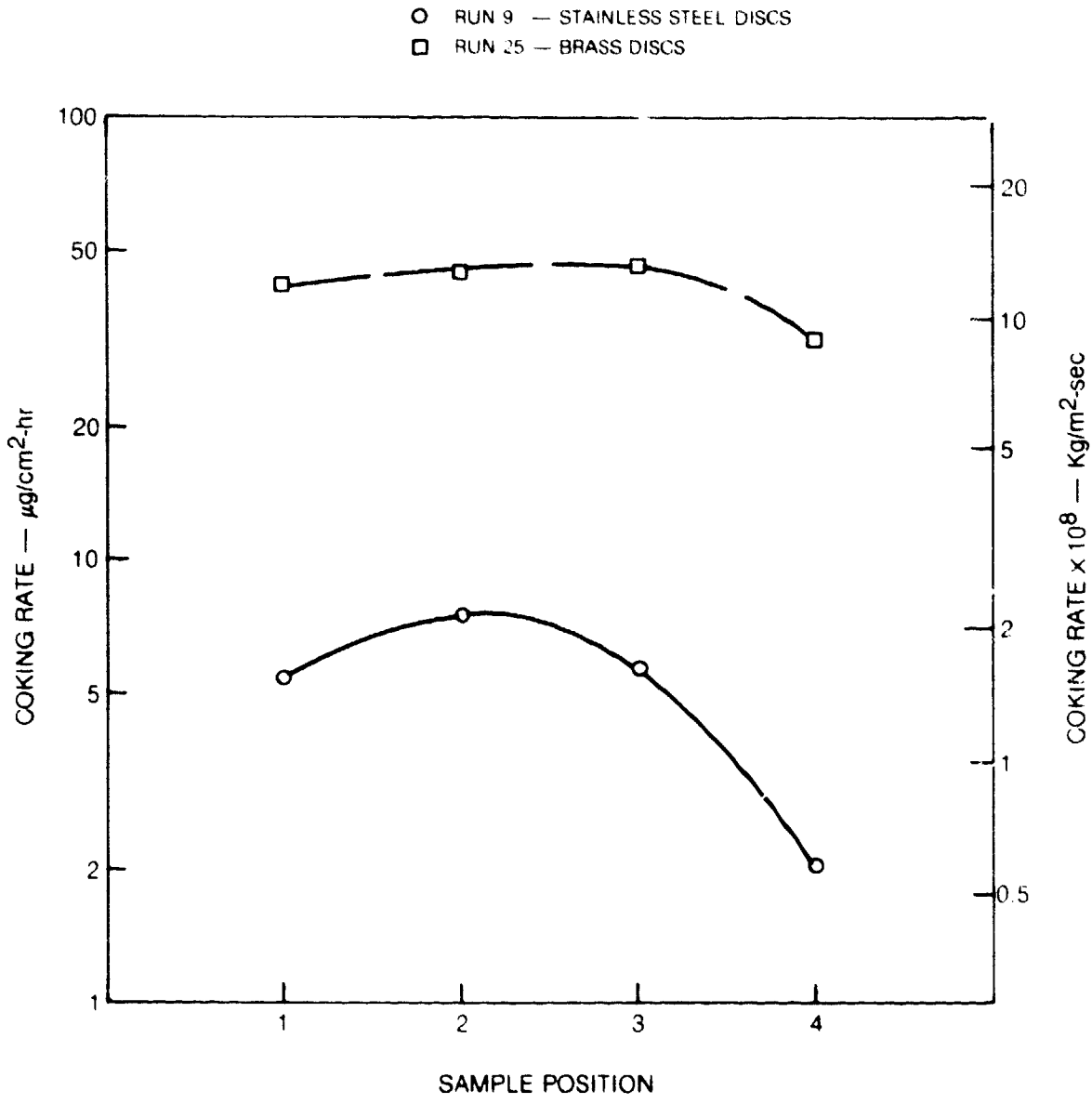

Figure 23. — Coking Rate on Brass and Stainless Steel Discs in Regular Diesel Fuel

ORIGINAL PAGE IS
OF POOR QUALITY

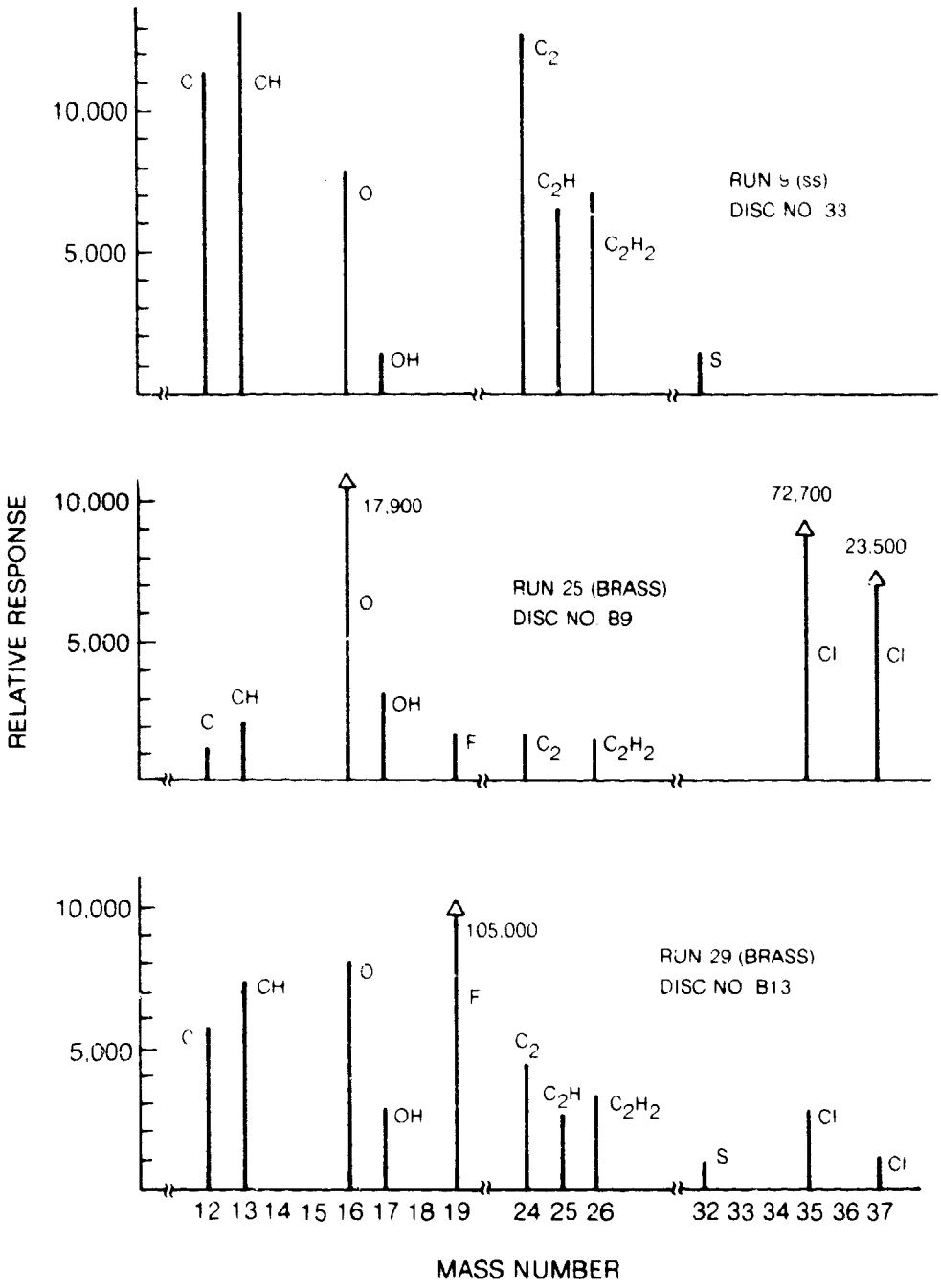

Figure 24. — Negative SIMS Analysis ($^{20}Ne^-$) of Deposits

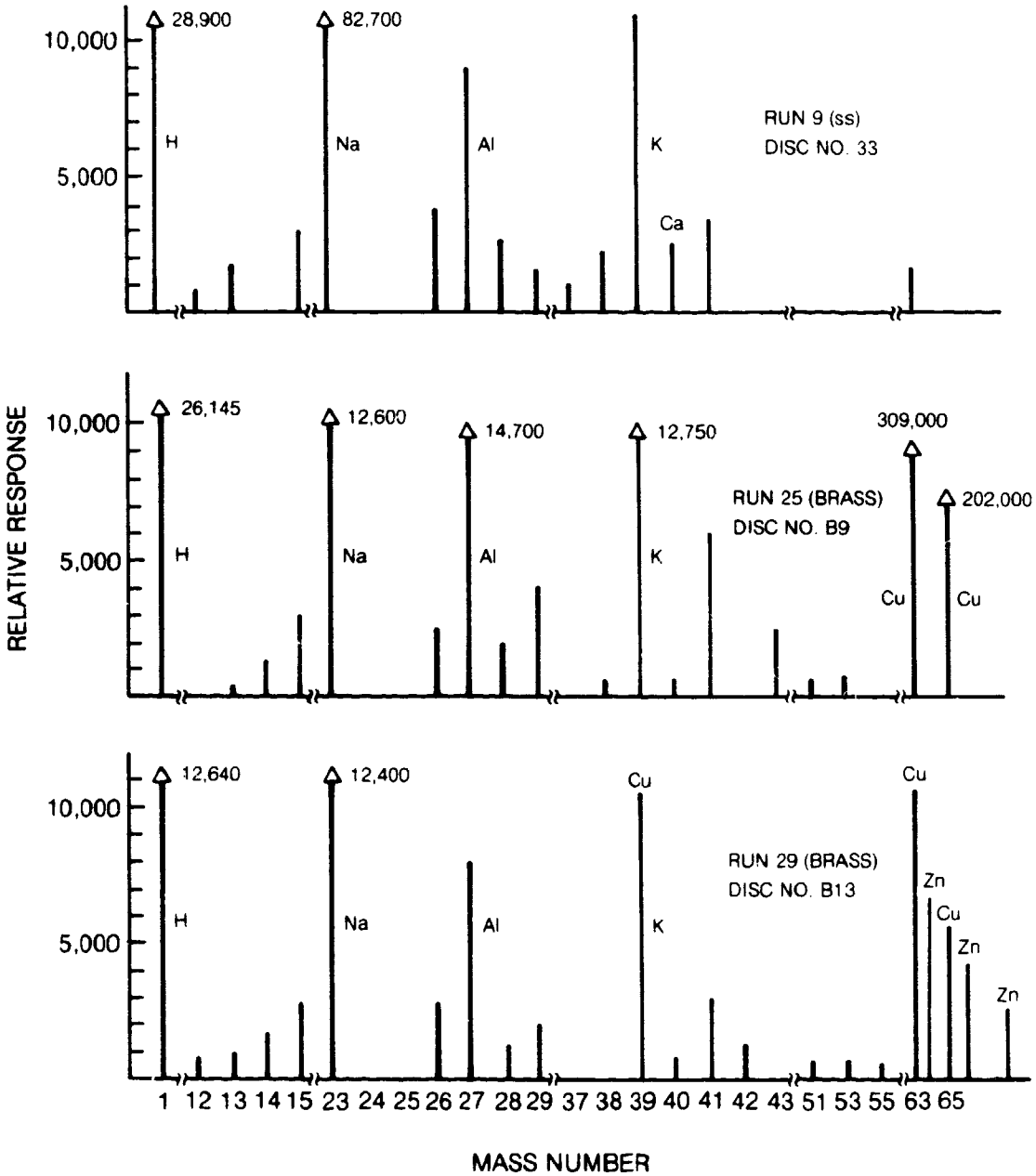

Figure 25. — Positive SIMS Analysis ($^{20}Ne^{+}$) of Deposits

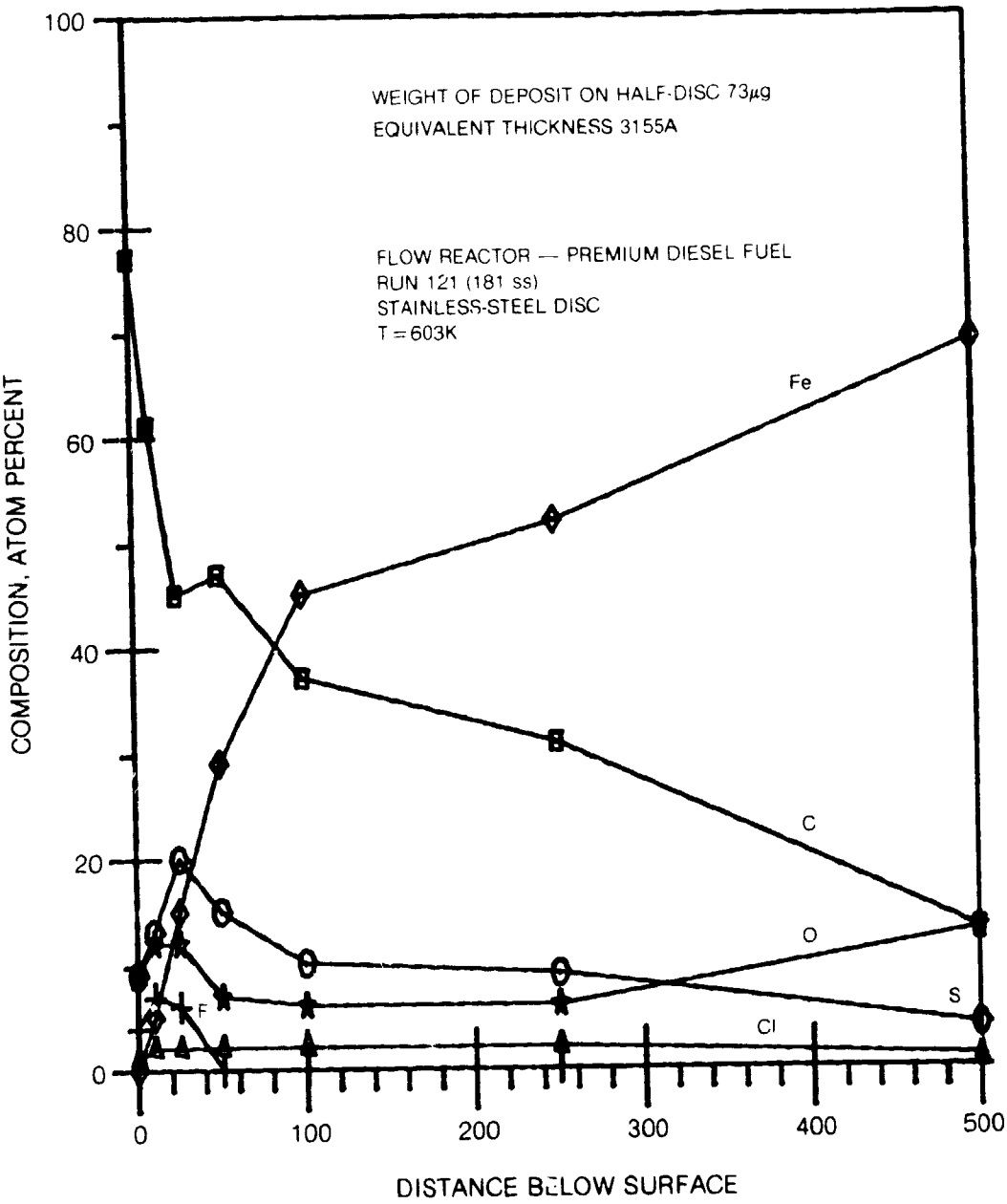

Figure 26A. — AES Analysis of Deposit on Paired Discs Stainless Steel in Premium Diesel Fuel

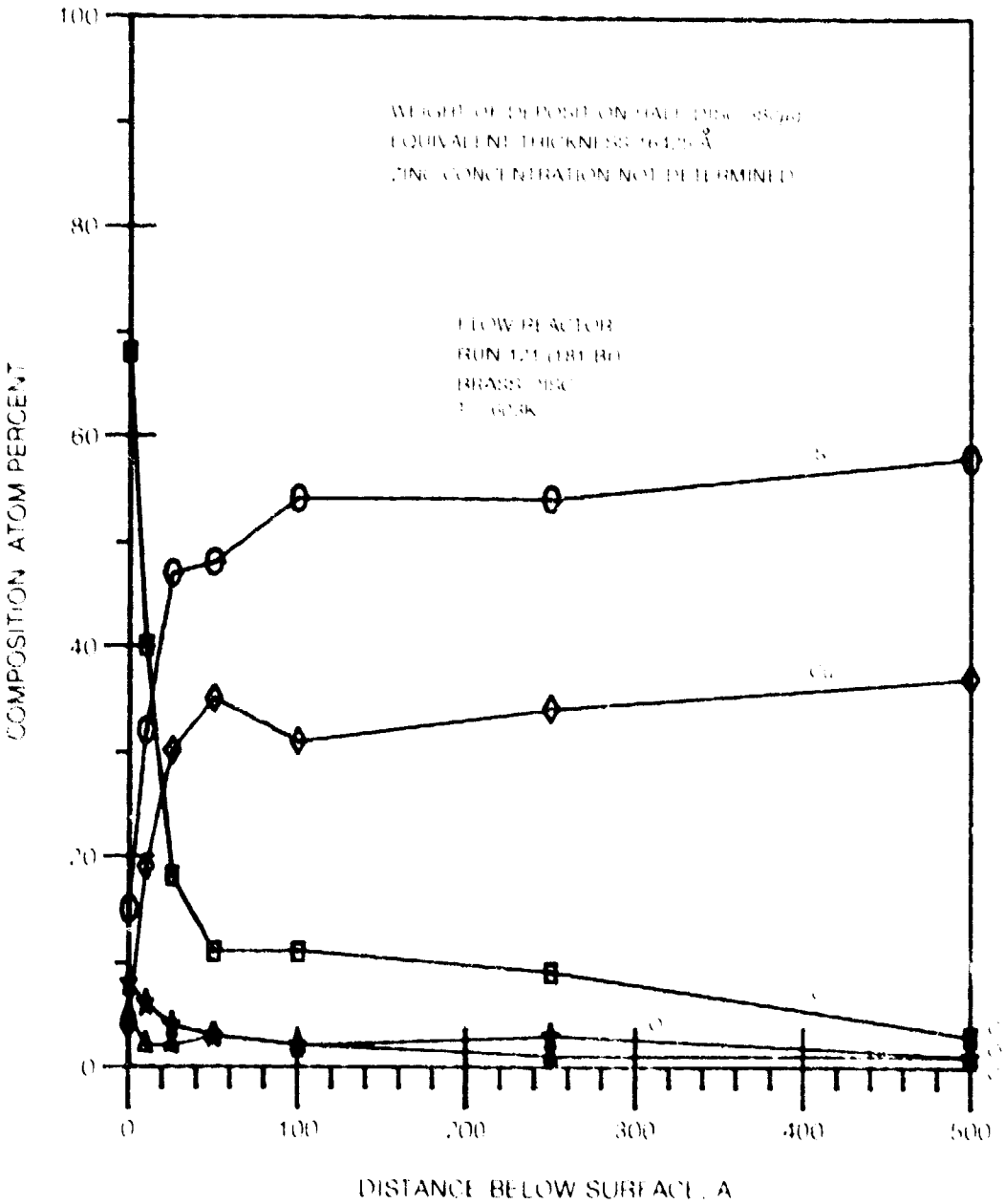

Figure 26B. — AES Analysis of Deposit on Paired Discs — B Brass in Premium Diesel Fuel

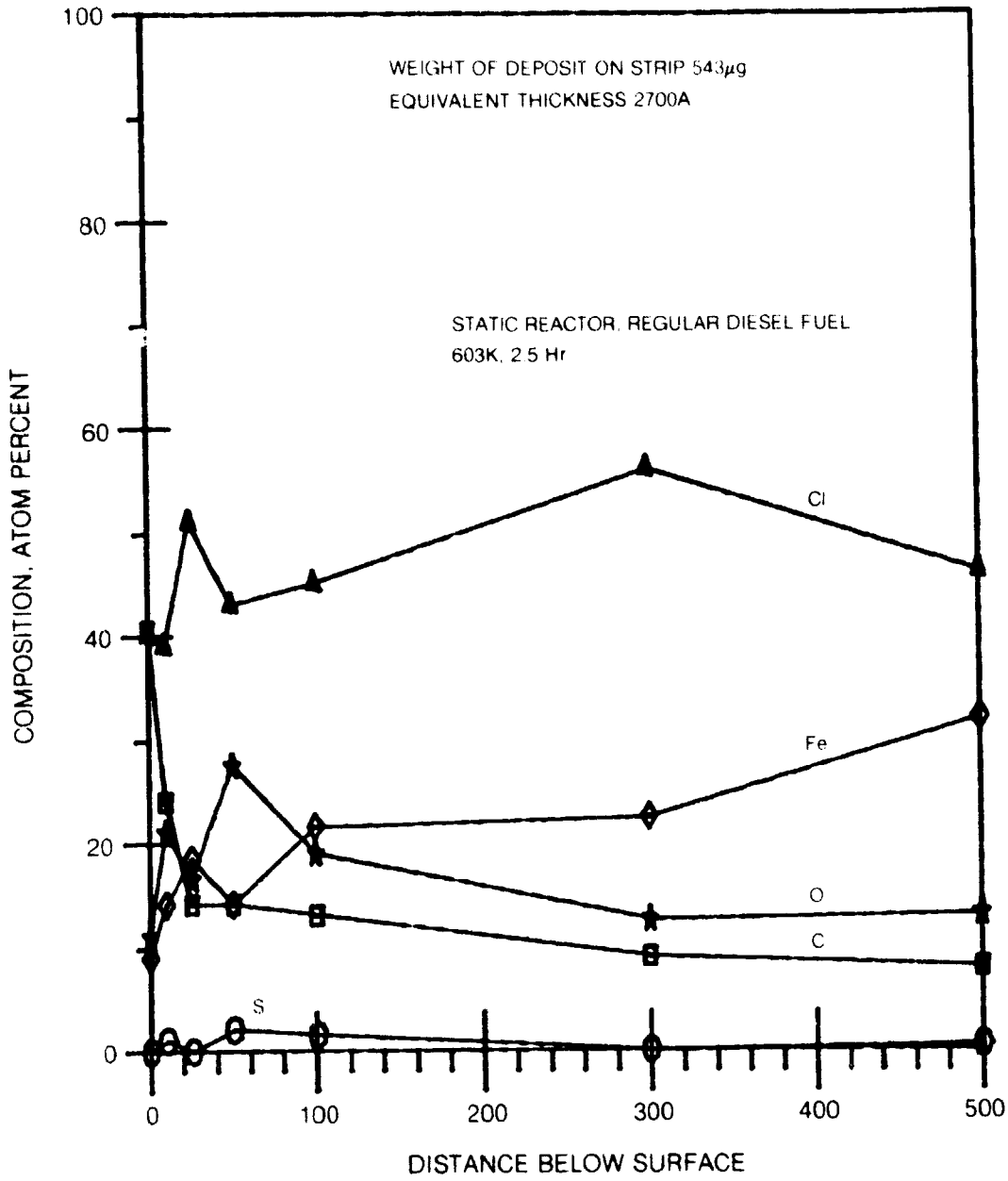

Figure 27. — AES Analysis of Deposit from Regular Diesel Fuel — Run 63 (New Tube and Strip)

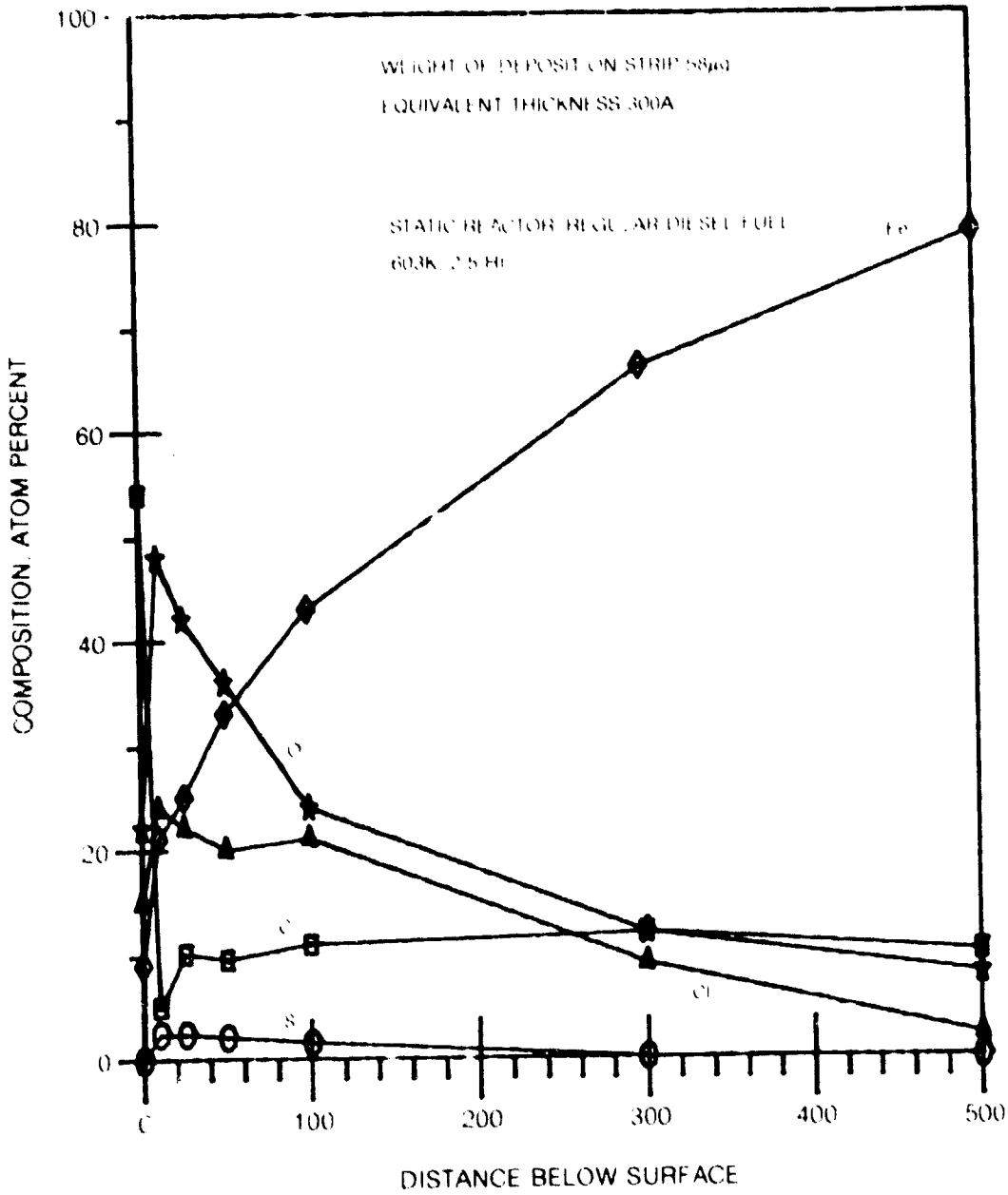

Figure 28. — AES Analysis of Deposit from Regular Diesel Fuel — Run 64 (Reused Tube, New Strip)

APPENDIX A

FUEL PROPERTIES

The two test fuels were characterized by ASTM procedures for aircraft turbine fuels. Results are given in Table A-1. For reference, the typical analysis of Jet A fuel is given.

The most-significant difference between the two fuels is in the aromatic content. The regular fuel was 47.84 percent aromatic; the premium fuel was 19.47 percent aromatic. Variation in other properties was small except for napthalenes (8.78 vs 4.21 percent). Distillation curves (especially near the end point) were very nearly the same, viscosities were essentially identical, and sulfur was similar (2037 vs 1758 ppm) and below the specification for Jet A (3000 ppm). Nitrogen was 219 vs 96 ppm.

The ASTM test of thermal stability (JFTOT) was also conducted. In these tests, the fuels exhibited similar properties, although the regular fuel (with higher aromatic, olefin, napthalene, nitrogen and sulfur content) was marginally more stable, giving slightly lower pressure drop at 473 F. In this test, both fuels closely matched the Jet A fuel used in the previous experiments (Ref. 1).

Doped fuels were prepared by adding research-grade quinoline, indole or benzoyl perioxide. Fuel specific gravity was assumed to be 0.84. Quinlone and indole were added to yield 1000 ppmW of nitrogen; 1 percent by weight benzoyl peroxide was added, yielding 1300 ppm of the peroxide oxygen. [On the basis of an analyzed fuel specific gravity of 0.87, actual concentration would be 3 percent lower.] The doped fuels were mixed and stored for use in a 20 gal drum.

TABLE A-1

PROPERTIES OF TEST FUELS

Composition	Regular Diesel	Premium Diesel	Jet A*
Aromatics, % Vol.	47.84	19.47	22.0
Olefins, % Vol.	1.23	0.70	0.3
Hydrogen, % Wt.	11.92	12.39	13.7
Naphthalenes, % Vol.	8.78	4.21	3.0
Sulfur, % Wt.	0.20	0.17	0.3
Nitrogen, % Wt.	0.02	0.01	0.001
Volatility			
Initial Distillation	461 K	451 K	444 K
10 percent	488 K	483 K	477 K
End Point	617 K	616 K	561 K
Physical Properties			
Viscosity, cs, 288 K	2.48	2.36	2.50
Specific Gravity, 288	0.8675	0.8308	0.82
Thermal Stability (JFTOT Test)			
Pressure Drop, mm at T(K)	1.0 (518)	1.5 (518)	25.0 (533)
(first test for Jet A-may be retested	0.0 (503)	1.0 (503)	
at 518K with limit of 25.0 mm)		0.0 (488)	
Deposit Code, rating at T(K)	4 (518)	4 (518)	3 (533)
(first test for Jet A-may be retested	2 (503)	3 (503)	
at 518K with limit of 3)		0 (488)	

*Specification or typical

APPENDIX B

DESCRIPTION OF ANALYTICAL TECHNIQUES

Auger Electron Spectroscopy

The Auger spectrometer provides identification of atoms within a thin layer (typically 15 Å) near the surface of a solid. A beam of energetic electrons is directed at the surface to be analyzed. These primary electrons excite atoms on the surface, and electrons from within the atoms are ejected. The Auger electrons have energies that are characteristics of the emitting atoms, and an energy analysis of the emitted electrons identifies individual species. Sensitivity varies with conditions; in the present case, sensitivities were of the order of 1%.

Although Auger analysis examines a thin layer (~ 15 Å), it is also possible to sputter (or remove) the surface atoms by bombarding the surface with energetic argon atoms and obtain concentration-depth profiles. For this work, atomic concentrations were determined over the range of 0 to 500 Å in depth. The efficiency of removal varies with species; particular atoms may selectively sputter off the surface, and some may redeposit onto the surface. The results are limited to trends, rather than absolute values, but depth profiles are useful in interpretation of data, especially from the static reactor, where deposits formed at early times may differ from those formed near the end of an experiment.

Typical raw data from the Auger spectrometer are shown in Figs. B-1 and B-2. Relative number concentrations are determined by dividing peak heights by the corresponding relative atomic sensitivities listed in Table B-1.

Ion Scattering Spectrometry/Secondary Ion Mass Spectometry (ISS/SIMS)

The 3M Model 520B ISS-SIMS provides two techniques for performing chemical analyses of surfaces. These are Ion Scattering Spectrometry (ISS) and Secondary (or Sputtered) Ion Mass Spectrometry (SIMS).

In ISS, a primary beam of ions (He^3 or Ne^{20}, for example) is directed at the surface to be studied at fixed energies. Some of these ions are scattered into an electrostatic energy analyzer mounted at a fixed angle relative to the incident ion beam. For low incident energies, the scattered ion current vs. scattered energy is characteristic of particular elements on the surface.

Some of the atoms and compounds sputtered from the surface by the primary beam are ionized, forming secondary ions, and these ions are analyzed in a mass spectrometer; this is the basis for SIMS. The secondary ion current vs. mass number identifies elements and compounds leaving the surface. Both the sputter yield and the degree of ionization depend on the ion being measured and on the properties of the substrate. As a consequence, reference standards are needed for quantitative results with SIMS. This is also true, though to a lesser extent, for ISS. For this work, no suitable reference standard was available; results obtained with this technique are predominately qualitative, and were used to verify major conclusions obtained using the Auger spectrometer.

Some special features of this instrument that distinguish it from Auger spectroscopy are: (1) it is sensitive only to the outer monolayer of the surface, (2) its sensitivity is as high as 1 part of a monolayer per million, (3) it can detect hydrogen and distinguish isotopes, and (4) it monitors both what is on the surfaces (ISS) and what is leaving the surface (SIMS).

Since the results from this machine are considered to be qualitative, data were only obtained at depths of 0 and 25 Å. The 25 Å depth was selected to be below atmospheric contamination; however, contamination on these samples was found at 25 to 50 Å.

TABLE B-1

RELATIVE AUGER SENSITIVITES OF
VARIOUS ELEMENTS

Element	Relative Sensitivity
C	0.20
N	0.32
O	0.50
F	0.48
Na	0.20
S	0.80
Cl	1.05
K	0.80
Ca	0.48
Fe	0.20
Cu	0.22

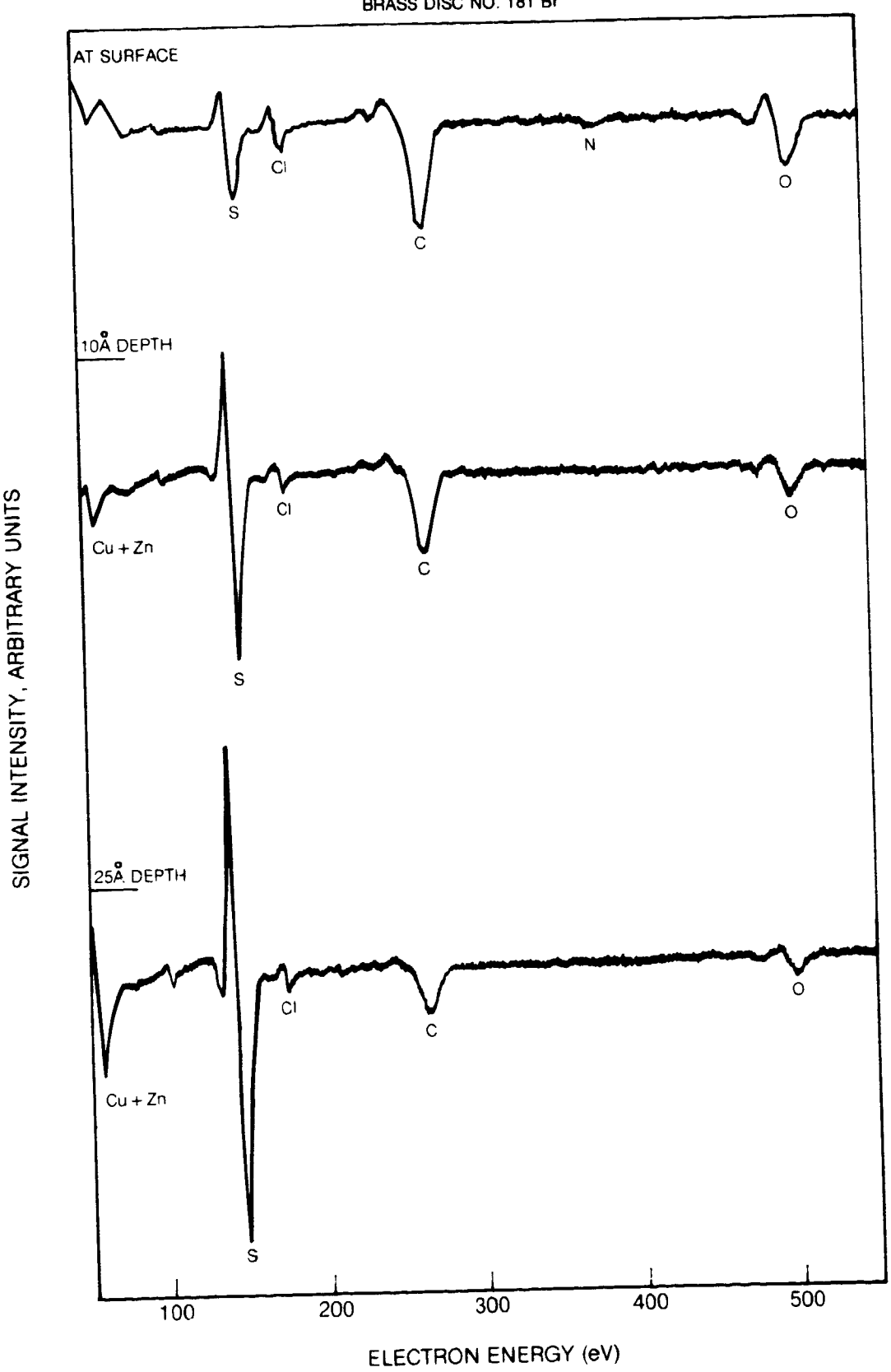

Figure B-1. — AES Raw Data for Run 121

82-11-53-13

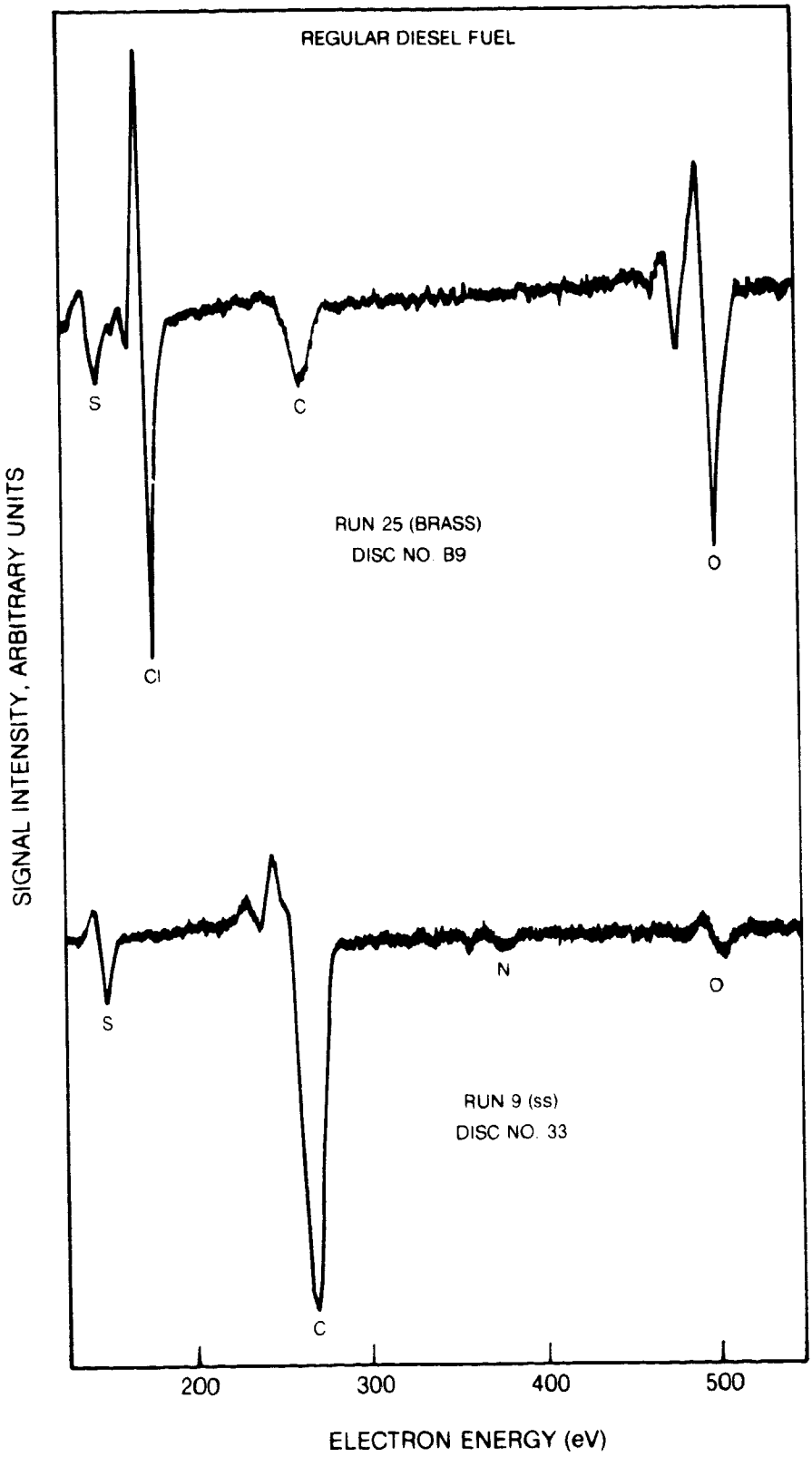

Figure B-2. — AES Raw Data at Depth of 10A

82-11-53-12

APPENDIX C

ESTIMATE OF FUEL TEMPERATURE RISE

The fuel temperature was measured at two locations in the fuel system simulator: within a short manifold upstream of the rectangular channel and at the end of the channel, just upstream of the restrictor nozzle. The entire profile of fuel temperature in the channel was calculated using correct fuel properties by a procedure used in other studies sponsored by NASA at UTRC (Ref. 1,3). Measured values were in qualitative agreement, but were somewhat higher, probably because of stagnation around the thermocouples.

The calculated profiles are shown in Fig. C-1; a summary of outlet temperatures for the various combinations of wall temperature and flow rate is given in Table C-1. The fuel residence time, based on volumetric flow (or on a constant fuel density) is also listed. Note that maximum bulk fuel temperature range from 141 to 581 F in this set of tests; residence time varies from 4 to 50 seconds.

The heating of fuel in the simulator is rather slow, because the flow tends to remain laminar as heat is added from the wall (Ref. 3), and transport is principally by diffusion. For the highest flow rate used in the calculations (12 gph at T_{wall} of 300 F), the outlet Reynolds number is approximately 35000. For a flow of 1 gph at T_{wall} of 625, the outlet Reynolds number is approximately 3000.

Although the run temperatures were selected in advance of the calculations presented here, it is worth noting that useful overlap in the fuel temperatures occurs. For example, the entire profile is the same for a flow of 2 gal/hr at 500 F or a flow of 4 gal/hr at 625 F. If the deposit formation depended only upon bulk fluid temperature, two such runs should have the same deposit weights and rates. Alternately, runs differing in flow rate at a fixed temperature should vary in proportion to residence time and to difference in fuel temperature. The observed variation is smaller than would be predicted on the basis of bulk-temperature dominance. This is discussed in more detail in the section on results.

TABLE C-1

APPROXIMATE RESIDENCE TIMES AND
OUTLET BULK FUEL TEMPERATURE

		T_{max} at T_{wall}, (deg F)			
$\dot{V}$, gph	t, sec	300	500	625	750
1	50	245	404	490	581
2	25	216	334	404	
4	12.5			334	
6	8.5		245		
12	4.3	141			

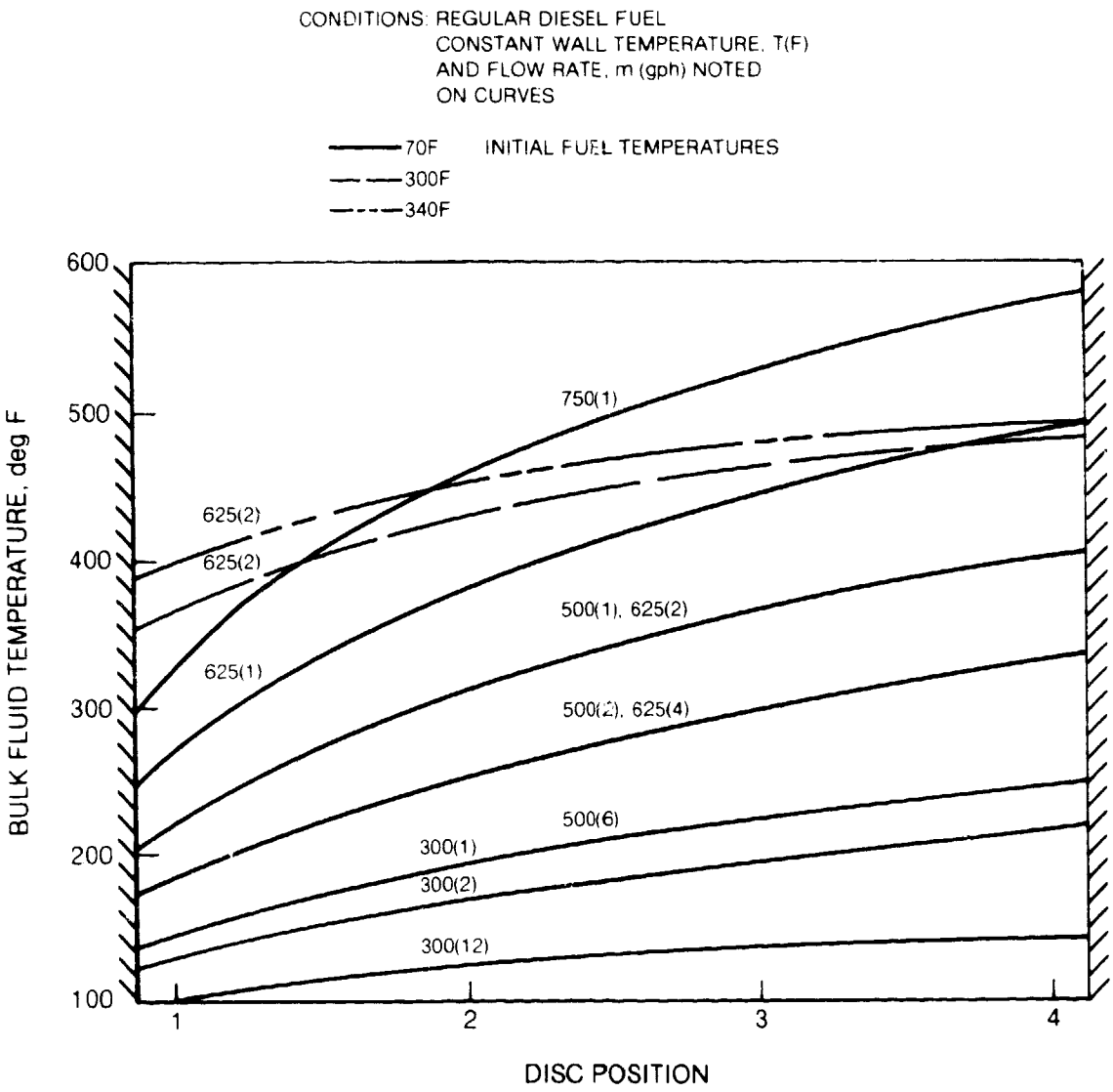

Figure C-1. — Calculated Fuel Temperature Profiles in Simulator System

82-11-53-14

END

DATE

FILMED

APR 14 1983